isvr Institute of Sound and Vibration Research

Investigation of the Mode Count of One-dimensional Systems

G. Xie, D.J. Thompson and C.J.C. Jones

ISVR Technical Memorandum No 882

February 2002

University of Southampton

SCIENTIFIC PUBLICATIONS BY THE ISVR

Technical Reports are published to promote timely dissemination of research results by ISVR personnel. This medium permits more detailed presentation than is usually acceptable for scientific journals. Responsibility for both the content and any opinions expressed rests entirely with the author(s).

Technical Memoranda are produced to enable the early or preliminary release of information by ISVR personnel where such release is deemed to the appropriate. Information contained in these memoranda may be incomplete, or form part of a continuing programme; this should be borne in mind when using or quoting from these documents.

Contract Reports are produced to record the results of scientific work carried out for sponsors, under contract. The ISVR treats these reports as confidential to sponsors and does not make them available for general circulation. Individual sponsors may, however, authorize subsequent release of the material.

UNIVERSITY OF SOUTHAMPTON

INSTITUTE OF SOUND AND VIBRATION RESEARCH

DYNAMICS GROUP

Investigation of the Mode Count of One-dimensional Systems

by

G. Xie, D.J. Thompson and C.J.C. Jones

ISVR Technical Memorandum No: 882

February 2002

Authorised for issue by
Dr M.J. Brennan
Group Chairman

ABSTRACT

The mode count of one-dimensional subsystems is investigated with particular reference to the relationship with the boundary conditions. The effects due to boundary conditions are found for both longitudinal and bending vibration of a single one-dimensional element. Each fixed boundary of a rod in longitudinal vibration reduces the average mode count by ½. Depending on the type of boundary, the average mode count of a beam in bending vibration is reduced by between 0 and 1 for each boundary. Then the mode count of a two-beam system is studied, where it is found that an intermediate constraint has the same effect on the average mode count as the same type of constraint applied at an end. The analysis is then extended to a multi-beam system. For either a finite periodic multi-beam system or a system with a number of randomly spaced constraints, both cases in a single line, the mode count of the whole system is found to follow the same average behaviour as the two-beam system. The mode count of the cross-section of an extruded plate is then investigated. An approximate method for the extruded section is developed based on the results for multi-beam systems and the results are compared with those from an FEM analysis. Finally the modal density and driving point mobility of the extruded section are also studied and it is shown that these can be estimated quite well from the above analysis.

CONTENTS

1 INTRODUCTION

The typical body structure of a modern railway carriage constructed of aluminium consists essentially of extruded plates. The extruded plate is an efficient structure that provides high strength and low weight, both of which are essential for the design of a high-speed passenger train. In applications, the extruded plates are subjected to dynamic excitations that may cause excessive internal noise levels unless an adequate study of vibration and sound transmission is performed at the design stage. However, until now, little work is available in this area. Geissler and Neumann [1] recently studied the acoustical properties of the extruded plate by using a calculation based on Statistical Energy Analysis (SEA). In their study using AutoSEA the sandwich flexible panel and the rib stiffened plate formulations are used to represent the vibro-acoustic behaviours of the extruded plate as a subsystem of the SEA model. The calculation results show considerable deviation from the measured data and the reasons are unknown.

In the case of a running train the possible sources of dynamic excitation cover a very wide frequency range and mainly include the rail-wheel excitation, engine excitation and boundary layer turbulence at high speeds. Therefore, understanding and studying the dynamic characteristics of the extruded plate over the main frequency range of the excitation is an important area where work is required.

Extruded plates cannot be regarded as finite 'periodic' structures because the spans between stiffeners are irregularly spaced. The example of an extruded plate used in the present work is the floor of a typical railway carriage, as shown in Figure 1.1. It consists of an upper plate, a lower plate and a set of stiffening plates set at angles between 33° and 49° and some at 90°. The work described in this report is concentrated on modelling the behaviour of the cross-section in the x-y plane as shown in Figure 1.2. This extruded section is composed of a set of one-dimensional segments so that the problem is converted to a study of one-dimensional components. The aim is to consider the extruded plate as a single system not as a series of connected susbsystems.

The aim of the present work is to investigate the mode count in undamped one-dimensional systems which can be used in the prediction for the extruded section. The mode count is a very important parameter in SEA because it represents the number of resonant modes available to

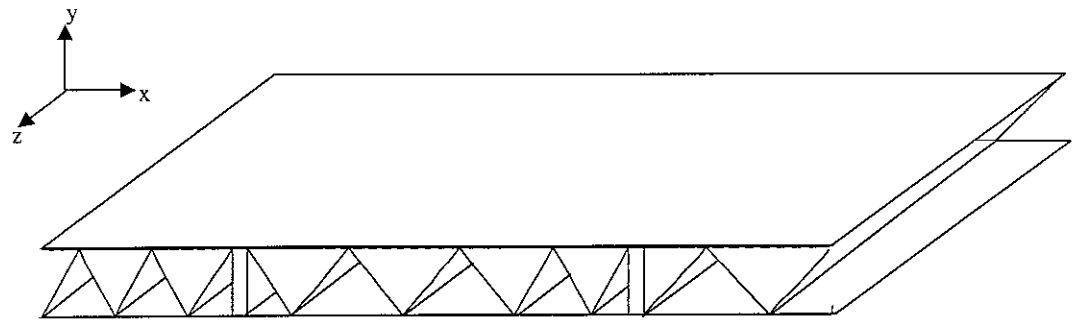

Figure 1.1 Example of an extruded plate (half of the floor).

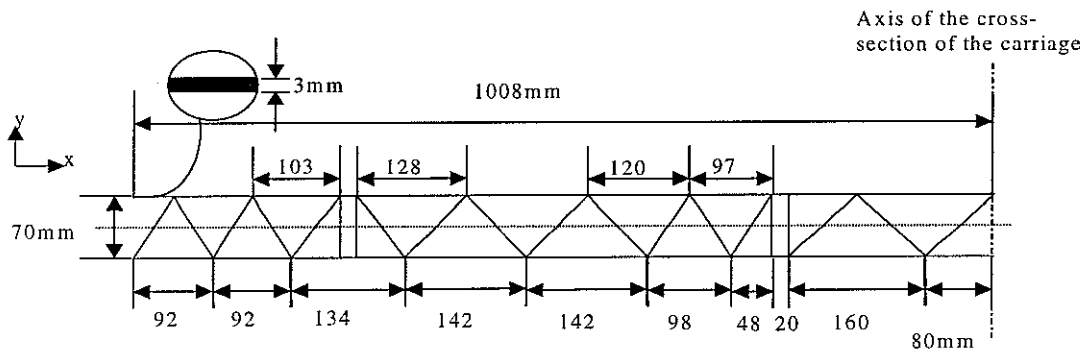

Figure 1.2 Cross-section of the extruded plate

receive and store energy in a system. A theoretical method of evaluating the mode count for extruded plates is of particular benefit when an SEA method is used to model the interior noise for railway vehicles. In Chapter 2, the relationship between the mode count of a single beam and the applied boundary conditions is investigated. In Chapter 3, a two-beam system with equal or unequal lengths is investigated. The relationship between the mode count of the two-beam system and the type of intermediate constraint applied is shown. This relationship is extended to a multi-beam system in Chapter 4. In section 4.1 and 4.2, a method of approximating the mode count of a finite periodic beam system is derived. It is shown that the mode count of a finite periodic system can be estimated by a simple formula in terms of the total length of beams and the number of constraints. In section 4.3, the mode count of a system of beams with random lengths is studied numerically using Finite Element Method (FEM) analysis. The same conclusion is obtained as for the periodic case. Finally in Chapter 5 these techniques are applied to the extruded section and the results are compared to those from an FEM analysis.

Equation Section 2

2 SINGLE ONE-DIMENSIONAL SYSTEM

2.1 NATURAL MODES

It is well known that natural modes of vibration occur in any finite continuous system. The number of modes occurring below a certain frequency f is called the mode count $N(f)$. The theoretical mode count for continuous systems can be obtained by combining boundary information with the dispersion relation for free waves in the system. Lyon and DeJong [2] give an expression for the mode count in terms of wavenumber:

$$N(k) = \frac{kL}{\pi} + \delta_{BC} \tag{2.1}$$

where δ_{BC} is dependent on the boundary conditions (and according to Lyon and DeJong is usually a constant of magnitude less than or equal to 1), L is the length of the one-dimensional system and k is the wavenumber which is related to frequency. For the particular wave type being considered, such as bending or longitudinal waves, the dispersion relation defines the frequency dependence of the wavenumber.

2.1.1 LONGITUDINAL MODES IN A ROD

The free longitudinal vibration in a bar is governed by the wave equation which is expressed as

$$\frac{\partial^2 u}{\partial x^2} - \frac{1}{c_L^{\,2}} \frac{\partial^2 u}{\partial t^2} = 0 \tag{2.2}$$

where c_L is the phase velocity of the longitudinal vibration. ($c_L = \sqrt{\frac{E}{\rho}}$ where E is Young's modulus and ρ is the density).

When the motion is harmonic at circular frequency $\omega=2\pi f$, the above equation can be expressed as the one dimensional *Helmholtz equation*

$$\frac{d^2 u(x)}{dx^2} + k^2 u(x) = 0 \tag{2.3}$$

where k is the wavenumber at a frequency ($k = 2\pi / wavelength = \omega / c_L$).

The general solution of the equation (2.3) is

$$u(x) = A_1 e^{jkx} + A_2 e^{-jkx} \tag{2.4}$$

To understand this solution physically, the two terms represent opposite-going propagating waves which are superposed. The propagating wave is characterized by the wavenumber k. This is the phase difference between two points in the continuous system at a unit distance apart in the direction of wave propagation. As the wave propagates, it can be said that its phase changes by k per unit length. At each of the boundaries, a phase difference is introduced between the incoming and reflected waves. The total phase change as the wave travels one complete circuit around the system can be expressed by

$$\varepsilon = -2kL + \varepsilon_L + \varepsilon_R \tag{2.5}$$

where ε_L and ε_R are the phase change at the left-hand and right-hand ends respectively.

The natural modes occur when the total phase change is equal to an integral number of 2π's. This principle is well known as the *phase-closure* principle (see [3]). From a knowledge of the wavenumber-frequency relationship as well as the phase change when a propagating wave impinges on each end-boundary of the system, the phase-closure principle can be used to find the natural frequencies. It is convenient to begin by considering the reflection coefficient of a propagating wave arriving at the end. Here, the term A_1 in equation (2.4) is supposed to be the incident wave and A_2 is supposed to be the reflected wave. The boundary is taken to lie at x=0.

For longitudinal vibrations in a rod, simple boundary conditions are either free or rigid at the two ends.

For free boundary conditions, the force must vanish. So $\left.\frac{du}{dx}\right|_{BC} = 0$, $A_1 = A_2$, and the phase change due to reflection is 0.

For fully fixed conditions, the displacement must vanish. So $u|_{BC} = 0$, $A_1 = -A_2$, and the phase change due to reflection is π.

The frequency equations of natural modes for different boundary conditions are now readily obtained by using the phase-closure principle.

- **Free-free**

The natural modes are governed by

$$-2kL+\varepsilon_L+\varepsilon_R=-2kL=-2(n-1)\pi$$

$$kL=(n-1)\pi \text{ for } n=1,2,\cdots \tag{2.6}$$

The result k=0 for n=1 corresponds to a rigid body mode.

- **Free-fixed**

The natural modes are governed by

$$-2kL+\varepsilon_L+\varepsilon_R=-2kL+\pi=-2(n-1)\pi$$

$$kL=(n-\frac{1}{2})\pi \text{ for } n=1,2,\cdots \tag{2.7}$$

- **Fixed-fixed**

The natural modes are governed by

$$-2kL+\varepsilon_L+\varepsilon_R=-2kL+\pi+\pi=-2(n-1)\pi$$

$$kL=n\pi \text{ for } n=1,2,\cdots \tag{2.8}$$

2.1.2 BENDING MODES IN A BEAM

The flexural wave equation for the wave displacement w in a uniform Euler-Bernoulli beam is

$$EI\frac{\partial^4 w}{\partial x^4}+\rho A\frac{\partial^2 w}{\partial t^2}=0 \tag{2.9}$$

where EI is the bending stiffness of the beam and ρA is the mass per unit length.

In the usual way, the general solution by the wave method has the form

$$w(x,t)=(A_1e^{kx}+A_2e^{-kx}+A_3e^{jkx}+A_4e^{-jkx})\exp(j\omega t). \tag{2.10}$$

where the four x-dependent terms in equation (2.10) are recognized in order as the positively growing evanescent wave, the decaying evanescent wave, the negatively propagating wave and the positively propagating wave. They will be referred to by their coefficients A_1, A_2, A_3 and A_4 respectively.

Applying the phase-closure principle requires a knowledge of the reflection coefficient at boundaries at which a wave arrives. For the bending vibration of a beam, four basic boundary conditions have to be considered: free, sliding, simple support and fully fixed. Except for the sliding boundary, the results of the other three have been presented by Mead [3]. For an incident

propagating wave A_4 arriving at the boundary, this is reflected into an evanescent wave A_1 and a propagating wave A_3. The total motion in the beam is

$$w(x) = A_1 e^{kx} + A_3 e^{jkx} + A_4 e^{-jkx} \tag{2.11}$$

which is illustrated in Figure 2.1.

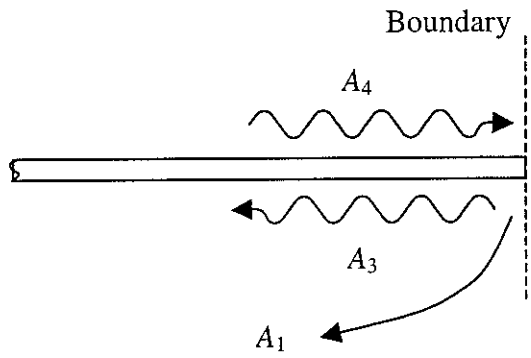

Figure 2.1 Illustration of the wave motion at boundary

For a free boundary condition, $\left.\frac{\partial^2 w}{\partial x^2}\right|_{BC} = 0$, $\left.\frac{\partial^3 w}{\partial x^3}\right|_{BC} = 0$, $A_3 = -jA_4$, $A_1 = (1-j)A_4$, and the phase change due to reflection is $-\pi/2$.

For a pinned (simple support) boundary condition, $w|_{BC} = 0$, $\left.\frac{\partial^2 w}{\partial x^2}\right|_{BC} = 0$, $A_3 = -A_4$, $A_1 = 0$, and the phase change due to reflection is π.

For a fully fixed boundary condition, $w|_{BC} = 0$, $\left.\frac{\partial w}{\partial x}\right|_{BC} = 0$, $A_3 = -jA_4$, $A_1 = -(1-j)A_4$, and the phase change due to reflection is $-\pi/2$.

For a sliding boundary condition, $\left.\frac{\partial w}{\partial x}\right|_{BC} = 0$, $\left.\frac{\partial^3 w}{\partial x^3}\right|_{BC} = 0$, $A_3 = A_4$, $A_1 = 0$, and the phase change due to reflection is 0.

The whole process of finding natural modes by using the phase-closure principle is quite simple when the evanescent waves arriving at and reflected from the boundaries are ignored. This is

almost exact for the third and higher order modes of simple beams and exact for the special case of a beam with simple supports or sliding boundary conditions at both ends [3]. Now the frequency equations for a single beam with different boundary conditions are readily obtained.

- **Free-free**

The natural modes are governed by

$$-2kL+\varepsilon_L+\varepsilon_R=-2kL-\pi/2-\pi/2=-2n\pi$$

$$kL=(n-\frac{1}{2})\pi. \tag{2.12}$$

To include two rigid modes by a rearrangement of n, equation (2.12) should be rewritten as

$$kL=(n-\frac{3}{2})\pi. \tag{2.13}$$

where $n = 3,4, \cdots\cdots$

- **Free-sliding**

The natural modes are governed by

$$-2kL+\varepsilon_L+\varepsilon_R=-2kL-\pi/2+0=-2n\pi$$

$$kL=(n-\frac{1}{4})\pi. \tag{2.14}$$

To include one rigid mode by a rearrangement of n, the item in the round bracket in (2.14) should reduced by 1. The final result is

$$kL=(n-\frac{5}{4})\pi. \tag{2.15}$$

where $n = 2,3,4, \cdots$.

- **Free-pinned**

The natural modes are governed by

$$-2kL+\varepsilon_L+\varepsilon_R=-2kL-\pi/2+\pi=-2n\pi$$

$$kL=(n+\frac{1}{4})\pi. \tag{2.16}$$

To include one rigid mode by a rearrangement of n, the item in the round bracket in (2.16) should reduced by 1. The final result is

$$kL=(n-\frac{3}{4})\pi. \tag{2.17}$$

where $n = 2,3,4, \cdots$.

- **Free-fixed**

The natural modes are governed by

$$-2kL+\varepsilon_L+\varepsilon_R=-2kL-\pi/2-\pi/2=-2n\pi$$

$$kL=(n-\frac{1}{2})\pi. \tag{2.18}$$

where n = 1,2,3,···.

The natural modes of other combinations of boundary conditions are given in Appendix A.

2.2 AVERAGE MODE COUNT

The mode count is the number of modes below a certain frequency. It consists of discrete numbers in reality. If it is plotted against frequency or wavenumber, a "staircase" curve appears as shown in Figure 2.2. For frequencies just below the n^{th} mode the mode count is n-1, just above the natural frequency it is n. A continuous function that approximates the average of the staircase function is more useful in practice (see Figure 2.2). This average function distributes the mode count along the wavenumber axis (or frequency axis). The average mode count can be represented by

$$N=n-\frac{1}{2} \tag{2.19}$$

at the resonance frequencies.

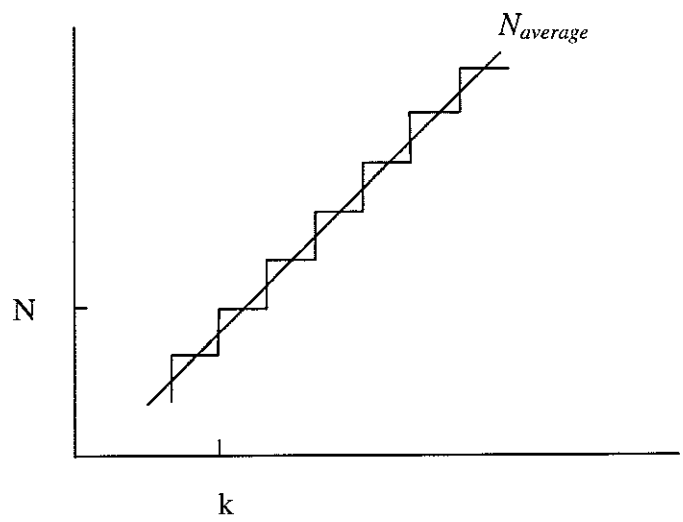

Figure 2.2. The illustration of the average mode count.

The concept of the average mode count will be used in the remainder of this report. When a mode count is mentioned, it normally means the average mode count function, not the discrete mode count.

2.3 RELATIONSHIP BETWEEN MODE COUNT AND BOUNDARY CONDITIONS

The mode count of natural modes can be easily obtained by rewriting the frequency equations in section 2.1 in the form of equation (2.1). Attention is required over the ambiguity in n. It is logical to follow the practice adopted above of making n start from 1 including the rigid body modes. Now the δ_{BC} in equation (2.1) can be readily obtained.

2.3.1 LONGITUDINAL MODE COUNT IN A ROD

By rewriting the frequency equation in section 2.1.1 for longitudinal motion in a rod, the average mode count in terms of the wavenumber can be expressed as

$$N = \frac{kL}{\pi} + \frac{1}{2} \qquad \text{for free-free boundary conditions,}$$

$$N = \frac{kL}{\pi} \qquad \text{for free-fixed boundary conditions,}$$

$$N = \frac{kL}{\pi} - \frac{1}{2} \qquad \text{for fixed-fixed boundary conditions.}$$

It can be noted that each fixed boundary constraint adds to the mode count by – ½ for longitudinal vibrations.

2.3.2 BENDING MODE COUNT IN A BEAM

By rewriting the frequency equation in section 2.1.2 for bending vibration in a beam, the mode count in terms of the wavenumber can be expressed as

$$N = \frac{kL}{\pi} + 1 \qquad \text{for free-free boundary conditions,}$$

$$N = \frac{kL}{\pi} + \frac{3}{4} \qquad \text{for free-sliding boundary conditions,}$$

$$N = \frac{kL}{\pi} + \frac{1}{4} \qquad \text{for free-pinned boundary conditions.}$$

$$N = \frac{kL}{\pi} \qquad \text{for free-fixed boundary conditions.}$$

By taking a free boundary as the base to compare the change of the mode count due to different boundary conditions, sliding adds the mode count by $-\frac{1}{4}$, pinned (simple support) condition by $-\frac{3}{4}$ and fixed boundary constraint by -1 for bending vibrations. This is found to apply to other combinations of boundary conditions as listed in Appendix A.

The mode count of the system can be obtained by considering the mode count of a free-free beam and the boundary conditions at two ends. It is given by

$$N = \frac{kL}{\pi} + 1 - \delta_L - \delta_R \tag{2.20}$$

where δ_L and δ_R are 0, ¼, ¾, and 1 corresponding to four boundary conditions respectively, as listed in Table 2.1. These values are used to find the constants δ_{BC} described in equation (2.1). δ_{BC} is given by

$$\delta_{BC} = 1 - \delta_L - \delta_R \tag{2.21}$$

Table 2.1 The constants subtracted from the mode count of a beam in bending for different boundary conditions

Boundary conditions	δ
Free	0
Sliding	¼
Pinned	¾
Fixed	1

2.3.3 GENERAL BOUNDARY CONDITIONS

Now more general boundary conditions are considered in which the end of the beam may be connected to a linear spring or a mass.

- **End spring**

When the end of a beam is constrained against transverse displacement by an elastic spring K, the resisting forces due to this spring is proportional to w. This resisting force is also balanced by the shear force at the end. Thus

$$EI\frac{\partial^3 w}{\partial x^3} = kw \tag{2.22}$$

Equation (2.22) gives

$$EIk^3(A_1 - jA_3 + jA_4) = K(A_1 + A_3 + A_4) \tag{2.23}$$

By introducing the non-dimensional stiffness coefficients $\sigma = K/EIk^3$, equation (2.23) can be rewritten as

$$(1-\sigma)A_1 + (-\sigma - j)A_3 + (-\sigma + j)A_4 = 0 \tag{2.24}$$

In addition, the bending moment must be zero. Hence $\left.\frac{\partial^2 w}{\partial x^2}\right|_{BC} = 0$, which gives

$$A_1 - A_3 - A_4 = 0 \tag{2.25}$$

From equation (2.24) and (2.25), a result can be obtained as follows

$$A_3 = -A_4\left(\frac{1-2\sigma+j}{1-2\sigma-j}\right) \text{ and } A_1 = -A_4\left(\frac{2j}{1-2\sigma-j}\right) \tag{2.26}$$

For the boundary condition of an end spring, the phase change is frequency dependent. When the frequency tends to zero, σ tends to infinity, $A_3 = -A_4$ and $A_1 = 0$. This is a pinned boundary condition. When the frequency becomes very large, σ tends to zero, $A_3 = -jA_4$ and $A_1 = (1-j)A_4$. This corresponds to a free boundary condition. Therefore the phase change due to an end spring would change from π at low frequency to $-\pi/2$ at high frequency. The amplitude reflection ratio can be expressed by

$$r = \frac{A_3}{A_4} = -\left(\frac{1-2\sigma+j}{1-2\sigma-j}\right) = e^{j\theta} \tag{2.27}$$

where $\theta = \tan^{-1}\left(\frac{2\sigma-1}{2\sigma(1-\sigma)}\right)$ and $-\frac{\pi}{2} \le \theta \le \pi$.

Consider a beam that is free at left-hand end and with a point spring at right-hand end. The natural modes can be found by

$$\begin{aligned} -2kL - \frac{\pi}{2} + \theta &= -2n\pi \\ kL &= (n - \frac{1}{4})\pi + \frac{\theta}{2} \end{aligned} \tag{2.28}$$

The rigid modes of a free-spring beam will consist of two (especially for $\sigma \to 0$), except one will have non-zero frequency. So in equation (2.28) n should be replaced by $n - 1$ and therefore can be rewritten as

$$kL = (n - \frac{5}{4})\pi + \frac{\theta}{2} \tag{2.29}$$

For $\sigma \to \infty$, $\theta \to \pi$ and $kL = (n - 3/4)\pi$, this is the case of a free-pinned beam.

For $\sigma \to 0$, $\theta \to -\pi/2$ and $kL = (n - 3/2)\pi$, this is the case of a free-free beam.

By comparing equation (2.29) with that of a free-free beam, the effect on the mode count of an end spring can be found as

$$\delta_{spring} = \frac{\theta}{2\pi} + \frac{1}{4} \tag{2.30}$$

δ_{spring} tends ¾ at low frequency and tends zero at high frequency. This is illustrated in Figure 2.3

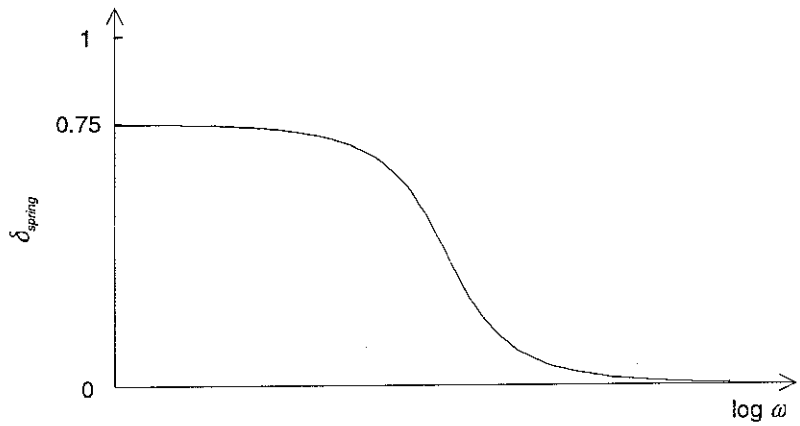

Figure 2.3 Illustration of δ_{spring} against frequency

- **End mass**

When the end of a beam undergoes a transverse displacement w, with acceleration $\partial^2 w/\partial t^2$, the resisting force due to an end mass m is proportional to $\partial^2 w/\partial t^2$. This resisting force is balanced by the shear force at the end. Thus

$$EI\frac{\partial^3 w}{\partial x^3} = m\frac{\partial^2 w}{\partial t^2} \tag{2.31}$$

Again the bending moment is zero, so equation can be used. Equation (2.31) gives

$$EIk^3(A_1 - jA_3 + jA_4) = -m\omega^2(A_1 + A_3 + A_4) \tag{2.32}$$

by writing $\mu = m\omega^2/EIk^3 = mk/\rho A$, equation (2.32) is expressed as

$$(\mu + 1)A_1 + (\mu - j)A_3 + (\mu + j)A_4 = 0 \tag{2.33}$$

From equation (2.25) and (2.33),

$$A_3 = -A_4\left(\frac{2\mu+1+j}{2\mu+1-j}\right) \text{ and } A_1 = -A_4\left(\frac{2j}{2\mu+1-j}\right) \tag{2.34}$$

From equation (2.34), it can be seen that the phase change due to an end point mass is dependent on frequency. When the frequency tends to zero, μ tends to zero, $A_3 = -jA_4$ and $A_1 = (1-j)A_4$. This is a free boundary condition. When the frequency tends to infinity, μ tends to infinity, $A_3 = -A_4$ and $A_1 = 0$. This is a pinned boundary condition. So the phase change due to an end mass would tends to $-\pi/2$ at low frequency and π at high frequency. However, if the reflection ratio is expressed as

$$r = \frac{A_3}{A_4} = -\frac{2\mu+1+j}{2\mu+1-j} = e^{j\theta} \tag{2.35}$$

it is found that θ moves through the third quadrant of the complex plane by $-\pi/2$ as frequency increases. Thus the phase change is actually from $-\pi/2$ to $-\pi$. This is different from the end spring when the total phase change is $-3\pi/2$.

Consider a beam that is free at left-hand end and with a point mass at right-hand end. The natural modes can be found by

$$\begin{aligned} -2kL - \frac{\pi}{2} + \theta &= -2n\pi \\ kL &= (n - \frac{1}{4})\pi + \frac{\theta}{2} \end{aligned} \tag{2.36}$$

It can be noted that there will always be two rigid body modes, even when mass is large. So equation (2.36) can be rewritten as

$$kL = (n - \frac{5}{4})\pi + \frac{\theta}{2} \tag{2.37}$$

For $\mu \to 0$, $\theta \to -\pi/2$ and $kL = (n-3/2)\pi$, this is the case of a free-free beam.

For $\mu \to \infty$, $\theta \to -\pi$ and $kL = (n-7/4)\pi$, this is different from the case of a free-pinned beam, which is governed by $kL = (n-3/4)\pi$. The reason is the second rigid body mode.

The effect of an end mass on the mode count can be obtained by

$$\delta_{mass} = \frac{\theta}{2\pi} + \frac{1}{4} \qquad -\pi \le \theta \le -\frac{\pi}{2} \tag{2.38}$$

δ_{mass} tends zero at low frequency and tends –¼ at high frequency. This is illustrated in Figure 2.4. It should be noted that δ for an end point mass is less than zero. This means that a mass is able to add to the mode count of a beam because it tends to lower the natural frequencies compared to a free end.

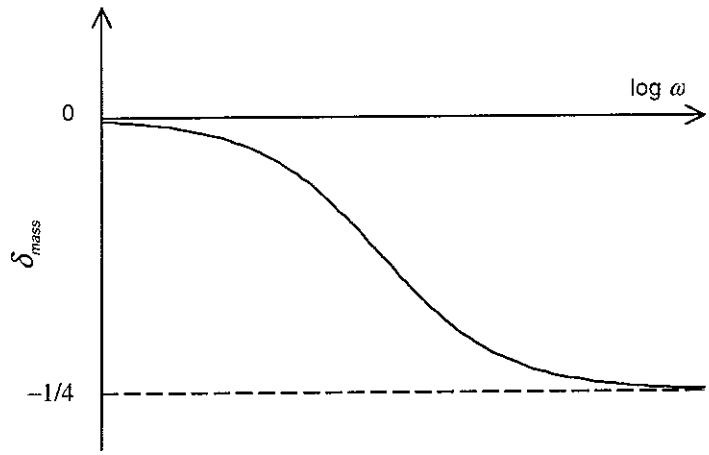

Figure 2.4 Illustration of δ_{mass} against frequency

Equation Section (Next)

3 TWO-BEAM SYSTEM

In chapter 2 the relationship between the mode count and boundary conditions for a single one-dimensional system has been discussed and the boundary dependent constants δ_L and δ_R have been obtained. In this chapter, the corresponding relationship for a one-dimensional system with an intermediate constraint will be considered. In other words, the system discussed is composed of two one-dimensional components, in particular two beams supporting bending vibrations, joined end to end. In the longitudinal case, an extra constraint can only be fully fixed, in which case the mode count becomes that of two uncoupled rods. The longitudinal case will not be discussed further since it is of less interest.

Consider a one-dimensional beam of length $2L$ with simple supports at the two ends. Another constraint is added at some intermediate point, not necessarily the centre (shown in Figure 3.1). What effect does this extra constraint have on the mode count of the system? How does this effect depend on the type of the constraint? The simplest case is to add an extra fixed condition into the system since the two sides of the fixed constraint will not be coupled with each other. This will be considered first.

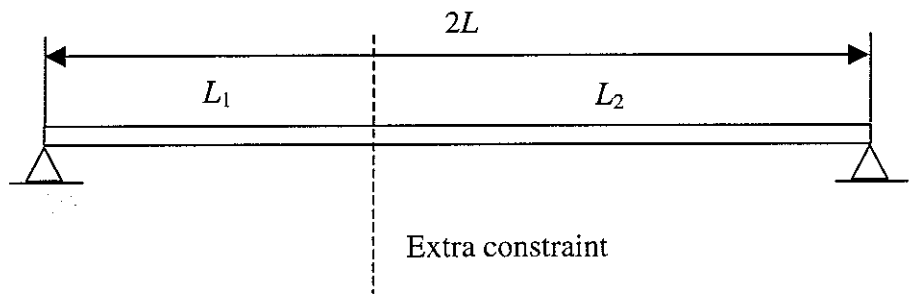

Figure 3.1. A simply supported beam of length $2L$ with an extra constraint.

3.1 A BEAM WITH AN INTERMEDIATE FIXED CONSTRAINT

If the extra constraint is a fixed condition, the system is then divided exactly into two independent single beams with pinned-fixed boundary conditions. The mode count for the whole system can be obtained by adding the two mode counts for the single beams

$$N_{total} = N_1 + N_2$$

$$N_{total} = \frac{kL_1}{\pi} - \frac{3}{4} + \frac{kL_2}{\pi} - \frac{3}{4}$$

$$N_{total} = \frac{2kL}{\pi} - \frac{1}{2} - 1 = N - 1 = N - \delta_{fixed} \qquad (3.1)$$

where N_{total} is the mode count of the whole system, N_1 and N_2 are the mode counts of the beams L_1 and L_2 respectively and N is the mode count of the original beam of length $2L$ without the extra intermediate constraint.

This shows that the mode count of the whole system can be estimated by taking the mode count of the system without the extra constraint and subtracting the coefficient $\delta = 1$ due to the fixed

boundary condition. A similar result is found for the trivial case of a 'free' intermediate boundary, for which $\delta_{free} = 0$.

The next question is whether the same is the case for an intermediate simple support or sliding support.

3.2 A BEAM WITH AN INTERMEDIATE SIMPLE SUPPORT CONSTRAINTS

3.2.1 GENERAL SOLUTION OF NATURAL MODES

Consider a one-dimensional system of length $2L$ with simple supports at the two ends (shown in Figure 3.1). Another simple support is applied at an arbitrary position between the two ends of the system. The left-hand and right-hand beams support waves represented as

$$w(x) = \begin{cases} Ae^{-jkx} + Be^{jkx} + Ee^{kx} \\ Ce^{-jkx} + De^{jkx} + Fe^{-kx} \end{cases} \tag{3.2}$$

in which the near-field waves at the two ends have been neglected. These component waves are illustrated in Figure 3.2.

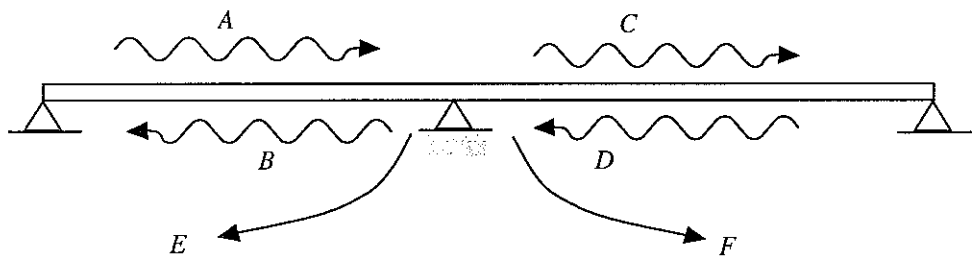

Figure 3.2 Diagram illustrating the component wave motions

If the near-field waves are neglected for determining the natural modes, the following four equations can be obtained.

$$A = r_L Be^{-2kL_1 j} \tag{3.3}$$

$$D = r_R Ce^{-2kL_2 j} \tag{3.4}$$

$$B = Dt_m + Ar_m \tag{3.5}$$

$$C = At_m + Dr_m \tag{3.6}$$

where r_L and r_R are amplitude reflection coefficients at the simple supports at the ends. From section 2.1.2, $r_L = -1$ and $r_R = -1$. t_m and r_m are the amplitude transmission and reflection coefficients at the middle simple support.

Substitute (3.3) and (3.4) into (3.5) and (3.6), then

$$B(1 - r_m r_L e^{-2kL_1 j}) = t_m r_R e^{-2kL_2 j} C \tag{3.7}$$

$$C(1 - r_m r_R e^{-2kL_2 j}) = t_m r_L e^{-2kL_1 j} B \tag{3.8}$$

In order to simplify (3.7) and (3.8) mathematically, it is convenient to write L_1=$L-l$, L_2=$L+l$, $\alpha = e^{-2klj}$ and $\beta = e^{-2klj}$. Then multiply the left-hand and right-hand sides of equation (3.7) and (3.8) respectively

$$BC(1 - r_m r_L \alpha / \beta)(1 - r_m r_R \alpha\beta) = BCt_m^2 r_R r_L \alpha^2 \tag{3.9}$$

t_m and r_m can be obtained by considering the continuity at the middle constraint. Taking this to be $x = 0$, the following conditions must be satisfied (here all the waves in equation (3.2) must be included).

$$w_-(0) = A + B + E = 0 \tag{3.10}$$

$$w_+(0) = C + D + F = 0 \tag{3.11}$$

$$w'_-(0) = w'_+(0) \qquad -jA + jB + E = -jC + jD - F \tag{3.12}$$

$$w''_-(0) = w''_+(0) \qquad -A - B + E = -C - D + F \tag{3.13}$$

Substitute (3.10) and (3.11) into the two sides of (3.13)

$$E = F \tag{3.14}$$

Substitute (3.10) and (3.11) into the two sides of (3.12)

$$-2jA + (1 - j)E = -2jD - (1 - j)E \tag{3.15}$$

If the beams were infinite in the right-hand direction, A would be the incident wave and D would not exist. Then

$$E = F = \frac{-1}{1 + j} A \tag{3.16}$$

Substitute (3.16) into (3.11)

$$C = \frac{1}{1 + j} A \tag{3.17}$$

Substitute (3.16) into (3.10)

$$B = \frac{-1}{1 - j} A \tag{3.18}$$

Thus the amplitude transmission coefficient

$$t_m = \frac{C}{A} = \frac{1}{1+j} \tag{3.19}$$

and the amplitude reflection coefficient

$$r_m = \frac{B}{A} = \frac{-1}{1-j} \tag{3.20}$$

Now substitute r_L, r_R, t_m and r_m into (3.9) and rearrange it to give

$$\alpha^2 - \frac{1-j}{2}\left(\frac{1}{\beta} + \beta\right)\alpha - j = 0 \tag{3.21}$$

Since $\frac{1}{\beta} + \beta = e^{2kl j} + e^{-2kl j} = 2\cos(2kl)$, equation (3.21) becomes

$$\alpha^2 - (1-j)\cos(2kl)\alpha - j = 0 \tag{3.22}$$

The roots of (3.22) have the form

$$\alpha = \frac{(1-j)\cos(2kl) \pm \sqrt{(1-j)^2\cos^2(2kl) + 4j}}{2} \tag{3.23}$$

Equation (3.23) is an irrational equation in k that gives a general solution for the natural frequencies of the two connected beams with simple support constraints. It can be noted that two sets of modes would occur in the system. A further simplification of equation (3.23) gives

$$e^{-2kLj} = \alpha = \frac{1-j}{2}\sqrt{1-\sin^2(2kl)} \pm \frac{1+j}{2}\sqrt{1+\sin^2(2kl)} \tag{3.24}$$

3.2.2 TWO IDENTICAL BEAMS

First, the situation is considered in which the extra constraint is located at the centre. In this case, l would be zero and the roots can be expressed as

$$\alpha_1 = 1 \text{ and } \alpha_2 = -j \tag{3.25}$$

The first root gives

$$e^{-2kLj} = 1 = e^{-2n\pi j}$$

so

$$kL = n\pi \tag{3.26}$$

These are exactly the modes of a pinned-pinned beam. In these modes the two beams vibrate in antiphase. This correspondes to a mode count $N_1 = \frac{kL}{\pi} - \frac{1}{2}$.

The second root gives

$$e^{-2kLj} = -j = e^{-(2n\pi+\frac{\pi}{2})j}$$

so

$$kL = (n+\frac{1}{4})\pi \tag{3.27}$$

These are exactly the modes of a fixed-pinned beam. In these modes the two beams vibrate in phase. This correspondes to a mode count $N_1 = \frac{kL}{\pi} - \frac{3}{4}$.

The total mode count of the system can be estimated by adding the two sets of modes together

$$N_{total} = N_1 + N_2$$

$$N_{total} = \frac{kL}{\pi} - \frac{1}{2} + \frac{kL}{\pi} - \frac{3}{4}$$

$$N_{total} = \frac{2kL}{\pi} - \frac{1}{2} - \frac{3}{4} = N - \frac{3}{4} = N - \delta_{pinned} \tag{3.28}$$

where N_{total} is the mode count of the whole system, N_1, N_2 are the mode counts of the antisymmetric and symmetric modes respectively and N is the mode count of the beam of length $2L$ without the extra intermediate constraint.

It is thus shown that the mode count of the whole system can be estimated by taking the mode count of the system without the extra constraint and subtracting the coefficient δ_{pinned} due to the simple support boundary condition. This is in the same as for the case of the fixed support in section 3.1.

3.2.3 ASYMMETRICAL SIMPLE SUPPORT

An asymmetrical intermediate simple support represents a more general case. By rechecking the general solution described in equation (3.24), the same conclusion is found.

The two roots in (3.24) can be expressed as

$$\alpha_1 = \frac{\sqrt{1-\sin^2(2kl)}+\sqrt{1+\sin^2(2kl)}}{2} + j\left(\frac{-\sqrt{1-\sin^2(2kl)}+\sqrt{1+\sin^2(2kl)}}{2}\right)$$
$$\alpha_2 = \frac{\sqrt{1-\sin^2(2kl)}-\sqrt{1+\sin^2(2kl)}}{2} + j\left(\frac{-\sqrt{1-\sin^2(2kl)}-\sqrt{1+\sin^2(2kl)}}{2}\right) \quad (3.29)$$

It can be noted that there is a relation between the two roots. Writing α_1 as $\alpha_1 = a + jb$, α_2 can be represented as $\alpha_2 = -b - ja$, where a and b are both positive. These two roots have the same modulus but different phase. It can be readily shown that the modulus is 1 in each case. Therefore the two roots can be represented as

$$\alpha_1 = e^{j\phi_1} \quad \alpha_2 = e^{j\phi_2} \quad (3.30)$$

where $0 \le \phi_1 \le \pi/2$ and $-\pi \le \phi_2 \le -\pi/2$.

The phases are related by

$$\phi_1 + \phi_2 = -\frac{\pi}{2} \quad (3.31)$$

Similar to the procedure taken in section 3.2.2, the first root gives

$$e^{-2kLj} = e^{j\phi_1} = e^{-(2n\pi-\phi_1)j},$$

so

$$kL = n\pi - \frac{\phi_1}{2} \quad (3.32)$$

The second root gives

$$e^{-2kLj} = e^{j\phi_2} = e^{-(2n\pi-\phi_2)j},$$

so

$$kL = n\pi - \frac{\phi_2}{2} \quad (3.33)$$

The total mode count of the system can be estimated by adding the two sets of modes together

$$N_{total} = N_1 + N_2$$
$$N_{total} = \left(\frac{kL}{\pi} - \frac{1}{2} + \frac{\phi_1}{2\pi}\right) + \left(\frac{kL}{\pi} - \frac{1}{2} + \frac{\phi_2}{2\pi}\right)$$
$$N_{total} = \frac{2kL}{\pi} - \frac{1}{2} + \left(\frac{\phi_1+\phi_2}{2\pi}\right) - \frac{1}{2} = N - \frac{3}{4} = N - \delta_{pinned} \quad (3.34)$$

where N_{total} is the mode count of the whole system, N_1 and N_2 are the mode counts of the two sets of modes and N is the mode count of the beam of length $2L$ without the extra middle constraint.

This shows that the average mode count of the whole system can be estimated in the same way as in section 3.2.2. The mode count of the system without the extra constraint is taken and the coefficient due to the simple support boundary condition, δ_{pinned}, is subtracted.

3.3 A BEAM WITH AN INTERMEDIATE SLIDING SUPPORT

Another case that could be considered is a two-beam system with a sliding support applied in the middle. The same definitions as in section 3.2.1 are used in this section. The free wave solution is represented by equation (3.2).

First, the amplitude transmission and reflection ratios can be found by taking account of the continuity at the sliding support. At $x = 0$, the following conditions must be satisfied.

$$w'_-(0) = -jA + jB + E = 0 \tag{3.35}$$

$$w'_+(0) = -jC + jD - F = 0 \tag{3.36}$$

$$w_-(0) = w_+(0) \qquad A + B + E = C + D + F \tag{3.37}$$

$$w'''_-(0) = w'''_+(0) \qquad jA - jB + E = jC - jD - F \tag{3.38}$$

Substitute (3.35) and (3.36) into the two sides of (3.38)

$$E = -F \tag{3.39}$$

Substitute (3.35) and (3.36) into the two sides of (3.37)

$$2A + (1+j)E = 2D + (1+j)F \tag{3.40}$$

If the beams were infinite in the right-hand direction, A would be the incident wave and D would not exist. Then

$$-E = F = \frac{1}{1+j}A \tag{3.41}$$

Substitute (3.41) into (3.36)

$$-jC = \frac{1}{1+j}A \tag{3.42}$$

Substitute (3.41) into (3.35)

$$B = \frac{1}{1+j}A \tag{3.43}$$

Thus the amplitude transmission coefficient

$$t_m = \frac{C}{A} = \frac{1}{1-j} \tag{3.44}$$

and the amplitude reflection coefficient

$$r_m = \frac{B}{A} = \frac{1}{1+j} \tag{3.45}$$

Substituting (3.44) and (3.45) into equation (3.9) gives

$$\alpha^2 + \frac{1+j}{2}\left(\frac{1}{\beta} + \beta\right) + j = 0 \tag{3.46}$$

The roots of equation (3.46) have the form

$$\alpha = \frac{-(1+j)\cos(2kl) \pm \sqrt{(1+j)^2\cos^2(2kl) - 4j}}{2} \tag{3.47}$$

Rearranging (3.47)

$$\alpha = \frac{-(1+j)}{2}\sqrt{1-\sin^2(2kl)} \pm \frac{1-j}{2}\sqrt{1+\sin^2(2kl)}\,, \tag{3.48}$$

thus

$$\begin{aligned} \alpha_1 &= \frac{-\sqrt{1-\sin^2(2kl)} + \sqrt{1+\sin^2(2kl)}}{2} + j\left(\frac{-\sqrt{1-\sin^2(2kl)} - \sqrt{1+\sin^2(2kl)}}{2}\right) \\ \alpha_2 &= \frac{-\sqrt{1-\sin^2(2kl)} - \sqrt{1+\sin^2(2kl)}}{2} + j\left(\frac{-\sqrt{1-\sin^2(2kl)} + \sqrt{1+\sin^2(2kl)}}{2}\right) \end{aligned} \tag{3.49}$$

If α_1 is written as $\alpha_1 = a - jb$, α_2 can be represented as $\alpha_2 = -b + ja$, where a and b are both positive. These two roots also have the same modulus but different phase in the complex plane. The phases are related by

$$\phi_1 + \phi_2 = \frac{\pi}{2} \tag{3.50}$$

Now the mode count for the system can be estimated.

$$N_{total} = N_1 + N_2 = \frac{kL}{\pi} - \frac{1}{2} + \frac{\phi_1}{2\pi} + \frac{kL}{\pi} - \frac{1}{2} + \frac{\phi_2}{2\pi} \tag{3.51}$$

$$N_{total} = \frac{2kL}{\pi} - \frac{1}{2} + \left(\frac{\phi_1 + \phi_2}{2\pi}\right) - \frac{1}{2} = N - \frac{1}{4} = N - \delta_{sliding} \tag{3.52}$$

This shows a result of the same form as the cases of simple support or fixed support located in the middle of the system.

3.4 A BEAM WITH A GENERAL INTERMEDIATE CONSTRAINT

Two general intermediate constraints, a point mass and a point spring, are now considered in this section.

3.4.1 INTERMEDIATE POINT MASS

Suppose that a point mass m is applied at an intermediate position between the two ends of the system. The free wave solutions of the system are still governed by equation (3.2). However, the amplitude transmission and reflection coefficient will become frequency-dependent. They can be obtained by considering the continuity of the position of the point mass. At $x = 0$, the following conditions must be satisfied:

$$w_-(0) = w_+(0) \qquad A + B + E = C + D + F \tag{3.53}$$

$$w'(0) = w'(0) \qquad -jA + jB + E = -jC + jD - F \tag{3.54}$$

$$w''_-(0) = w''_+(0) \qquad -A - B + E = -C - D + F \tag{3.55}$$

$$EI\left[w'''_-(0) - w'''_+(0)\right] = -m\omega^2 w(0) \qquad jA - jB + E - jC + jD + F = -\mu(A + B + E) \tag{3.56}$$

where $\mu = m\omega^2 / EIk^3 = mk / \rho A$ is non-dimensional parameter.

From (3.53) and (3.55), $E = F$. Equation (3.54) can be rewritten as

$$-jA + jB + 2E = -jC + jD \tag{3.57}$$

Substitute (3.57) into (3.56)

$$(4 + \mu)E = -\mu(A + B) \tag{3.58}$$

If the beams were infinite in the right-hand direction, A would be the incident wave and D would not exist. Then from (3.53),

$$A + B = C \tag{3.59}$$

Therefore

$$E = \frac{-\mu}{4 + \mu} C \tag{3.60}$$

Multiply the two sides of equation (3.55) with j and combine it with (3.54)

$$jA = jC + E \tag{3.61}$$

Substitute (3.60) into (3.61), the transmission ratio t_m can be found as

$$t_m = \frac{C}{A} = \frac{(4 + \mu)j}{(4 + \mu)j - \mu} \tag{3.62}$$

Then from (3.59) the reflection ratio r_m can be obtained as

$$r_m = \frac{B}{A} = \frac{\mu}{(4+\mu)j - \mu} \tag{3.63}$$

Since μ is a frequency-dependent parameter, the coefficients t_m and r_m are not constant. When frequency is very low, μ tends to zero, $t_m \to 1$ and $r_m \to 0$. This means that there is no constraint applied. Waves will propagate through the mass without reflection. When frequency is very high, μ tends to infinity, $t_m \to \frac{1}{1+j}$ and $r_m \to \frac{1}{j-1}$. This is the case of a simple support constraint (see section 3.2).

In order to know the effect of an intermediate spring on the mode count of the whole system, the solution of the natural frequencies must be found. By substituting the transmission and reflection ratio into equation (3.9), the natural frequencies can be found from

$$(r_m^2 - t_m^2)\alpha + r_m(\beta + \frac{1}{\beta})\alpha + 1 = 0 \tag{3.64}$$

Equation (3.64) can be simplified if the two beams are identical. In this case,

$$(r_m^2 - t_m^2)\alpha + 2r_m\alpha + 1 = 0 \tag{3.65}$$

Thus the roots of (3.65) are

$$\alpha_1 = -\frac{1}{r_m + t_m} \text{ and } \alpha_2 = -\frac{1}{r_m - t_m} \tag{3.66}$$

Substituting of (3.62) and (3.63) gives

$$\alpha_1 = \frac{\mu - (4+\mu)j}{\mu + (4+\mu)j} \text{ and } \alpha_2 = 1 \tag{3.67}$$

It may be noted from this that one set of modes (the antisymmetric modes) will always be the modes of a pinned-pinned beam whereas the other set of modes will depend on the mass and on frequency.

The first root gives

$$e^{-2kLj} = \frac{\mu - (4+\mu)j}{\mu + (4+\mu)j} = e^{j\phi_1} = e^{-(2n\pi - \phi_1)j} \tag{3.68}$$

where $\phi_1 = \tan^{-1}\left(\frac{\mu(4+\mu)}{4(\mu+2)}\right)$ and $\pi \le \phi_1 \le \frac{3\pi}{2}$. So the natural modes are governed by

$$kL = n\pi - \frac{\phi_1}{2} \tag{3.69}$$

and the mode count for this set of modes is

$$N_1 = \frac{kL}{\pi} - \frac{1}{2} + \frac{\phi_1}{2\pi} \tag{3.70}$$

The second root gives

$$N_2 = \frac{kL}{\pi} - \frac{1}{2} \tag{3.71}$$

The total mode count of the system can be estimated by adding the two sets of modes together

$$N_{total} = N_1 + N_2 = \frac{kL}{\pi} - \frac{1}{2} + \frac{\phi_1}{2\pi} + \frac{kL}{\pi} - \frac{1}{2}$$

$$N_{total} = \frac{2kL}{\pi} - \frac{1}{2} + \frac{\phi_1}{2\pi} - \frac{1}{2} = N + \frac{\phi_1}{2\pi} - \frac{1}{2} \tag{3.72}$$

Therefore the effect of an intermediate mass on the mode count of the system can be obtained by

$$\delta = \frac{1}{2} - \frac{\phi_1}{2\pi} \qquad \pi \le \phi_1 \le \frac{3\pi}{2} \tag{3.73}$$

For $\mu \to 0$, $\phi_1 \to -\pi$ and $\delta \to 0$; for $\mu \to \infty$, $\phi_1 \to -\pi/2$ and $\delta \to -¼$. This is the same as the case of a mass at the ends of the beams described in section 2.3.3. However, it must be indicated that δ for a mass at the ends of the beams is different from that at intermediate at a specific frequency, although they have same tendency to change along frequency axis. This can be seen when they are plotted against frequency. Figure 3.3 illustrates their differences. It can be shown that δ_{mass} for an intermediate mass is equivalent to δ_{mass} for an end mass in which μ is replaced by $\mu/4$.

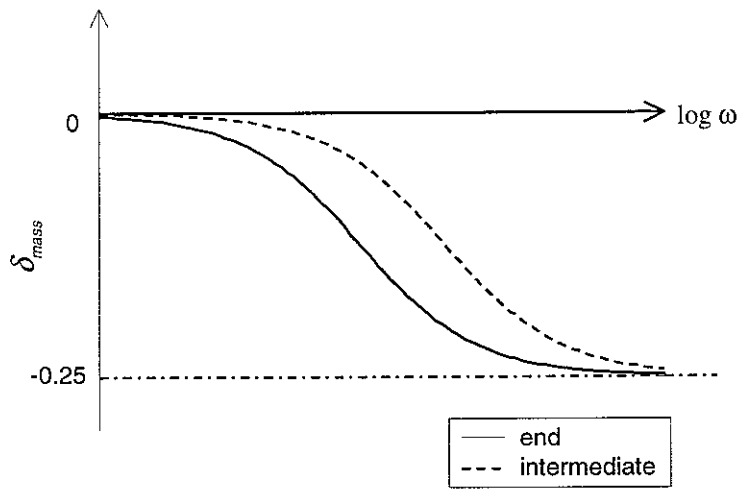

Figure 3.3 Difference between δ_{mass} at ends and for intermediate position on beams.

It can be seen that the intermediate point mass has a similar effect as that a point mass applied at the end of a beam, which is discussed in section 2.3.3. The difference in the mode count between a beam with and without an intermediate point mass is frequency-dependent, not constant. The mode count of the system with an intermediate point mass can be expressed by

$$N_{total} = N - \delta_{mass} \tag{3.74}$$

where N is the mode count of the beam without the intermediate mass and δ_{mass} is frequency-dependent parameter between zero to – ¼ as described in equation (3.73).

3.4.2 INTERMEDIATE POINT SPRING

When an intermediate point spring K is considered, the continuity conditions are mostly the same as the case of a point mass except for equation (3.56). The continuity of the shear force should be written as

$$EI\left[w_-'''(0) - w_+'''(0)\right] = Kw(0) \qquad jA - jB + E - jC + jD + F = \sigma(A + B + E) \tag{3.75}$$

where $\sigma = K/EIk^3$ is a non-dimensional stiffness coefficient.

The transmission and reflection ratios are now readily obtained by substituting σ into equation (3.62) and (3.63) to replace μ. For this case, t_m and r_m are

$$t_m = \frac{C}{A} = \frac{(4-\sigma)j}{(4-\sigma)j + \sigma} \tag{3.76}$$

$$r_m = \frac{B}{A} = \frac{-\sigma}{(4-\sigma)j + \sigma} \tag{3.77}$$

It can be found that an intermediate point spring has the same effect on the wave propagation as the end point spring discussed in section 2.3.3. At very low frequency, σ tends to infinity, $t_m \to \frac{1}{1+j}$ and $r_m \to \frac{1}{j-1}$. This is the case of a simple support constraint. At very high frequency, σ tends to zero, $t_m \to 1$ and $r_m \to 0$. This is the case of a free condition. Waves will propagate past the spring without reflection.

In order to know the effect of an intermediate spring on the mode count of the whole system, the solution of the natural frequencies must be found. By substituting the transmission and reflection ratio into equation (3.9), the natural frequencies can be found in

$$(r_m^2 - t_m^2)\alpha + r_m(\beta + \frac{1}{\beta})\alpha + 1 = 0 \tag{3.78}$$

Equation (3.78) can again be simplified if the two beams are identical. In this case,

$$(r_m^2 - t_m^2)\alpha + 2r_m\alpha + 1 = 0 \tag{3.79}$$

Thus the roots of (3.79) are

$$\alpha_1 = -\frac{1}{r_m + t_m} \text{ and } \alpha_2 = -\frac{1}{r_m - t_m} \tag{3.80}$$

Substituting of (3.76) and (3.77) gives

$$\alpha_1 = \frac{\sigma + (4-\sigma)j}{\sigma - (4-\sigma)j} \text{ and } \alpha_2 = 1 \tag{3.81}$$

It may be noted from this that one set of modes will always be the modes of a pinned-pinned beam whereas the other set of modes will depend on the stiffness and on frequency.

The first root gives

$$e^{-2kLj} = \frac{\sigma + (4-\sigma)j}{\sigma - (4-\sigma)j} = e^{j\phi_1} = e^{-(2n\pi - \phi_1)j} \tag{3.82}$$

where $\phi_1 = \tan^{-1}\left(\frac{\sigma(4-\sigma)}{4(\sigma-2)}\right)$ and $-\frac{\pi}{2} \le \phi_1 \le \pi$. So natural modes are governed by

$$kL = n\pi - \frac{\phi_1}{2} \tag{3.83}$$

and the mode count for this set of modes is

$$N_1 = \frac{kL}{\pi} - \frac{1}{2} + \frac{\phi_1}{2\pi} \tag{3.84}$$

The second root gives

$$N_2 = \frac{kL}{\pi} - \frac{1}{2} \tag{3.85}$$

The total mode count of the system can be estimated by adding the two sets of modes together

$$N_{total} = N_1 + N_2 = \frac{kL}{\pi} - \frac{1}{2} + \frac{\phi_1}{2\pi} + \frac{kL}{\pi} - \frac{1}{2}$$

$$N_{total} = \frac{2kL}{\pi} - \frac{1}{2} + \frac{\phi_1}{2\pi} - \frac{1}{2} = N + \frac{\phi_1}{2\pi} - \frac{1}{2} \tag{3.86}$$

Therefore the effect of an intermediate spring on the mode count of the system can be obtained by

$$\delta = \frac{1}{2} - \frac{\phi_1}{2\pi} \qquad -\frac{\pi}{2} \le \phi_1 \le \pi \tag{3.87}$$

For $\sigma \to \infty$, $\phi_1 \to \pi$ and $\delta \to$ ¾; For $\sigma \to 0$, $\phi_1 \to -\pi/2$ and $\delta \to 0$. This is the same as the case of a spring at the ends of the beams described in section 2.3.3. As for the mass discussed above, there is some difference for δ between at ends and at intermediate of the beams. This is illustrated in Figure 3.4; the two expressions for δ_{spring} can be shown to the equivalent if K is replaced by $K/4$ in δ_{spring} for the end spring.

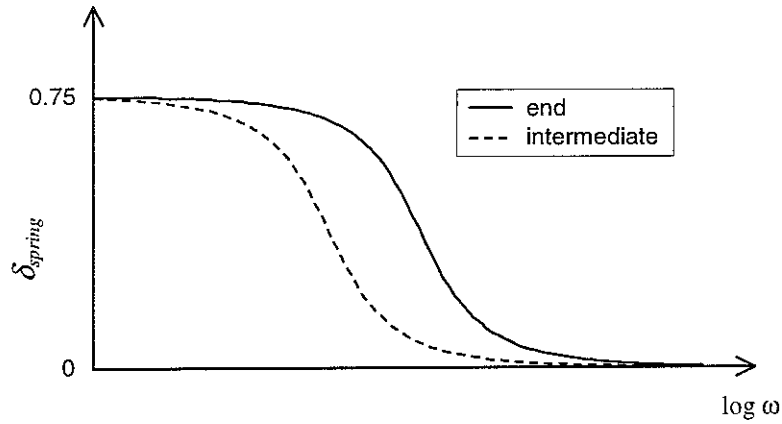

Figure 3.4 Difference between δ_{spring} at ends and for intermediate position on beams

The mode count of a beam with an intermediate point spring can thus be expressed by

$$N_{total} = N - \delta_{spring} \tag{3.88}$$

where N is the mode count of the beam without the intermediate spring and δ_{spring} is the frequency-dependent parameter described in (3.87).

3.5 CONCLUSION

Based on the analysis described in section 3.1 to 3.3, it can be concluded that the mode count of a beam with an extra intermediate constraint is equal to the mode count of this beam without any extra constraint, modified by a constant that depends only on the type of the constraint. These constants are normally the same as those applying for constraints at the ends of the beams described in Chapter 2 (Table 2.1). For a mass or a stiffness, the constants have a frequency dependent effect which is the same as for an end constraint apart from a constant factor.

Equation Section (Next)

4 MULTI-BEAM SYSTEM

This chapter will extend the conclusion obtained from two-beam systems to systems consisting of more beams. A finite periodic beam system will be discussed first and then a random multi-beam system will be considered.

4.1 FINITE PERIODIC BEAM SYSTEM

The finite periodic beam system discussed here is a finite length beam supported at regular intervals. The mode count of the system will be analysed by treating it as a long beam simply supported at two ends with a number of extra uniform intermediate constraints.

If $m-1$ equally spaced fixed constraints are applied, the system can be regarded as two pinned-fixed beams and $m-2$ fixed-fixed beams. The mode count of the whole system can be calculated by

$$N_{total} = 2N_{pinned-fixed} + (m-2)N_{fixed-fixed} \tag{4.1}$$

$$N_{pinned-fixed} = \frac{kL}{\pi} - \frac{3}{4} \tag{4.2}$$

$$N_{fixed-fixed} = \frac{kL}{\pi} - 1 \tag{4.3}$$

where N_{total} is the mode count of the whole system. $N_{pinned\text{-}fixed}$ is the mode count of a pinned-fixed beam. $N_{fixed\text{-}fixed}$ is the mode count of a fixed-fixed beam. m is the number of beam segments of the system. This yields

$$N_{total} = \frac{mkL}{\pi} - \frac{1}{2} - (m-1) = N - (m-1)\delta_{fixed} \tag{4.4}$$

where N is the mode count of the long beam with simple supports at the two ends.

Since fixed constraints separate the system into exactly uncoupled segments, the mode count for the whole system is readily obtained. It can be represented by the mode count of a long beam minus the product of the number of constraints (m – 1) and the constraint constant δ. It can also be noted that the same result could be obtained for the case of random (unequally spaced) constraints.

A more complicated case is that with simply supported constraints. This will be discussed in following sections.

4.2 SIMPLY SUPPORTED FINITE PERIODIC BEAM SYSTEM

4.2.1 NATURAL MODES AND MODE COUNT

Mead [4,5] gives a detailed study of the natural modes of a finite periodic system. The natural modes only occur in propagation bands that are described in terms of "bounding frequencies". The bounding frequencies depend on the natural frequencies of an individual segment of the system, with appropriate boundary conditions. These govern the upper and lower limits of the propagation bands. In the present case, the pinned-pinned and fixed-fixed boundary conditions are appropriate. The natural frequencies for pinned-pinned boundary conditions are obtained from

$$kL = n\pi \tag{4.5}$$

and for fixed-fixed boundary condition from

$$kL \approx (n+\frac{1}{2})\pi\,. \tag{4.6}$$

The propagation bands occur in the ranges $[n\pi, (n+1/2)\,\pi]$ where n is an integer starting from 1. m modes are available in each propagation band. Hence it can be seen that

between kL=0 and π, there are 0 modes,

between kL=π and $3\pi/2$, there are m modes,

between kL=$3\pi/2$ and 2π, there are 0 modes,

between kL=2π and $5\pi/2$, there are m modes

and so on.

Figure 4.1 shows an illustration of the mode count for the finite periodic beams system.

The average mode count can be obtained by finding the equation of a straight line passing through points that are located midway between the last mode in a propagation band and the first mode in the next propagation band. The physical explanation of these specific points is that the wavenumber at these points should be midway between the two wavenumbers at which two successive modes occur. In fact, these points are located in stop bands. Clearly this average mode count is only an approximation to the actual mode count, where modes tend to be clustered.

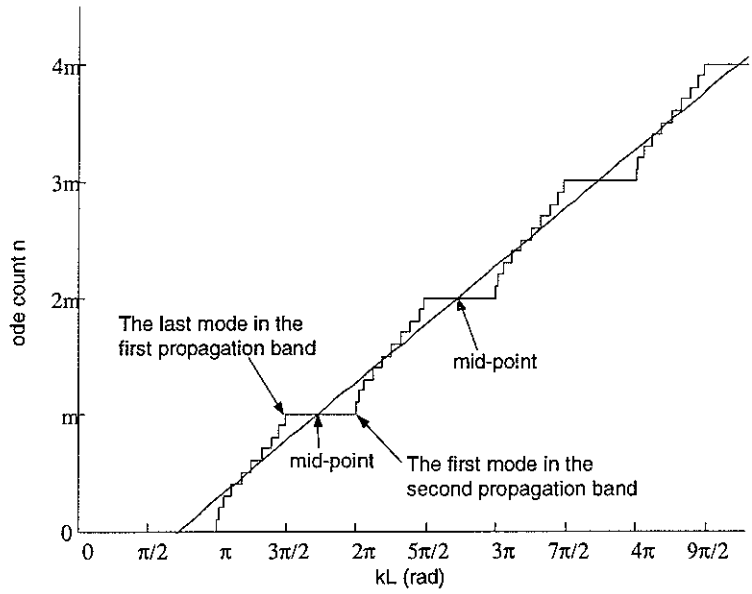

Figure 4.1 Illustration of the mode count of a finite periodic structure

The last mode in the first propagation band occurs approximately at $kL = \pi + \frac{(m-1)\pi}{2m}$. This is less than the bounding frequency since the end conditions of the whole beam are simple supports. The first mode in the second propagation band occurs at $kL=2\pi$. The mid-point is then located at $kL = \frac{(7-1/m)}{4}\pi$, which corresponds the mode count of m. The slope of the straight line is m/π. Therefore the average mode count of the finite periodic system can be represented as

$$N_{periodic} = \frac{m}{\pi}\left(kL - \frac{(7-1/m)}{4}\pi\right) + m = \frac{mkL}{\pi} - \frac{3}{4}(m-1) - \frac{1}{2} \tag{4.7}$$

$$N_{periodic} = N - (m-1)\delta_{pinned} \tag{4.8}$$

This shows that the finite periodic beams system has a mode count that can be estimated by the mode count of the long beam minus the product of the number of constraints (m – 1) and the constraint constant δ.

4.2.2 CASE STUDY

A beam of total length 2m, first with 5 identical segments and then with 10 identical segments, is studied in this section. Simple supports are applied at uniform intervals. The mode counts for the two cases are plotted in Figure 4.2. The mode count of the long beam itself is also plotted in the same figure for comparison.

The staircases plotted in Figure 4.2 are obtained from an FEM model using ANSYS. In the FEM model a number of beam elements are used adequately to approximate the behaviour of each beam segment. The maximum element length is 0.01m. The difference between the results for the periodic case and the average results for the long beam is plotted in Figure 4.3. There are a lot of fluctuations in these difference curves. However, the averaged values for 5 and 10 segments are 3 and 6.8, which are equal to those calculated by equation (4.8).

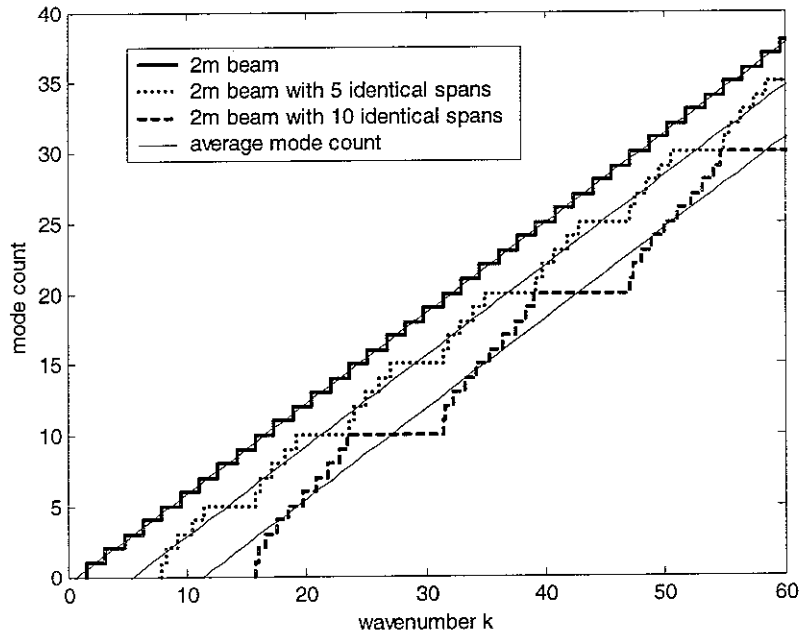

Figure 4.2. Mode count of periodic beams systems

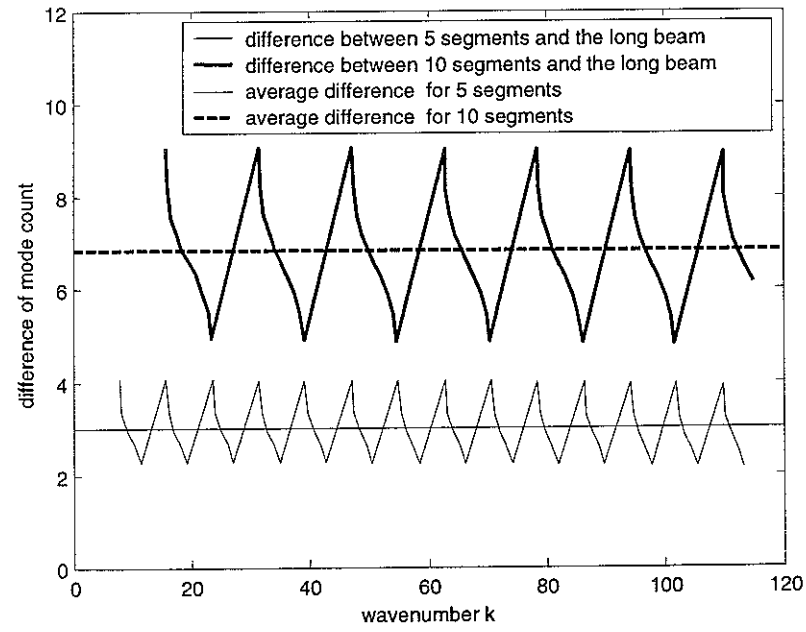

Figure 4.3. Differences of the mode count between the periodic and the long beam.

4.3 RANDOMLY SPACED MULTI-BEAM SYSTEM

The periodic structure is an ideal assumption suitable to be analysed theoretically. Real structures, however, might not be ideally periodic. Whether or not the conclusion based on the analysis of a finite periodic system can be extended to random multi-beam systems should therefore be considered for practical applications. Since it is nearly impossible to conduct an analytical investigation of the random multi-beam system, numerical tools such as FEM become appropriate. By reusing the example in section 4.2.2 but modifying the locations of the pinned constraints to make the periodic system non-periodic, the natural frequencies and average mode count can be calculated. The length of the segment is listed in Table 4.1. Figure 4.4 shows the mode count of the system with 10 random segments along with that with 10 periodic segments. This shows that the propagation and stop bands for the periodic system disappear. In fact the modes become local. The mode count difference between the random multi-beam system and the average result for the long beam is calculated and presented in Figure 4.5. The average value is equal to that of the periodic system.

This section therefore concludes with an estimated formula for the mode count of a multi-beam system without analytical proof but which has been demonstrated by the example shown. Equation (4.9) gives this estimated formula that has the same form as described in equation (4.8).

$$N_{random} = N - (m-1)\delta_{pinned} \tag{4.9}$$

Table 4.1 The length of the segment for the random multi-beam system used in FEM

Length of segment (m)
0.20
0.22
0.18
0.17
0.23
0.20
0.19
0.25
0.15
0.21
Total: 2m

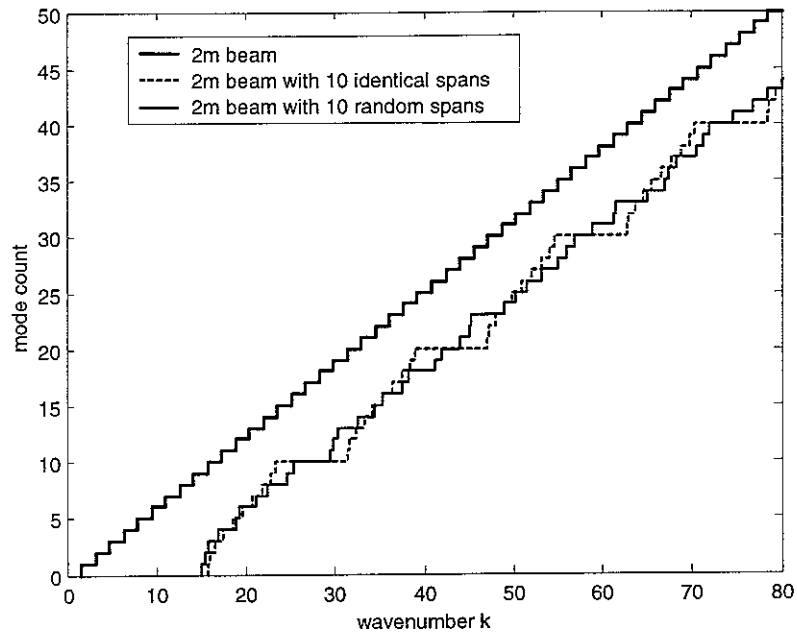

Figure 4.4. Mode counts of multi-beam systems

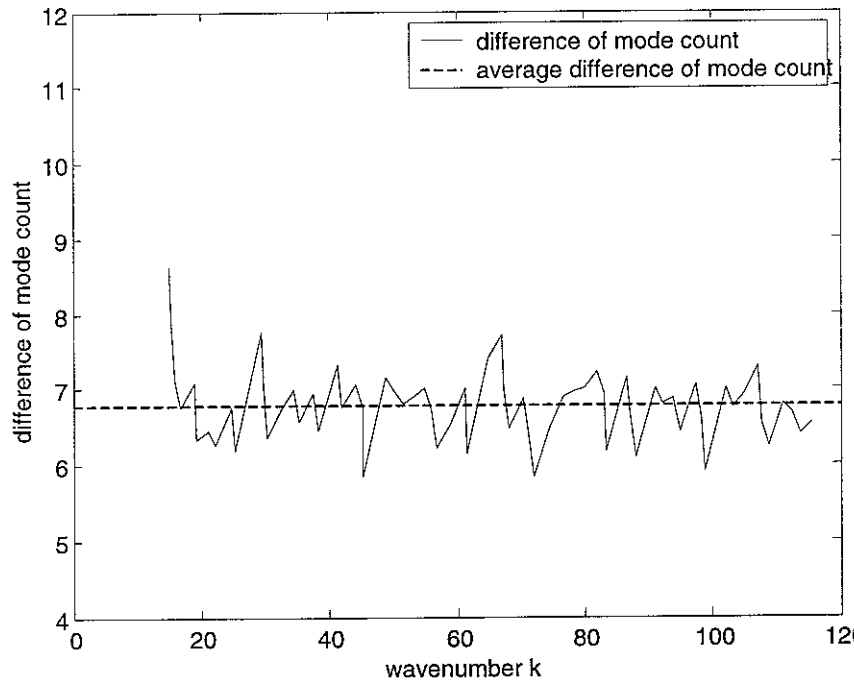

Figure 4.5 Mode count difference between the random multi-beam system and the result for the long beam

4.4 CONCLUSION

The mode count of a multi-segment one-dimensional system has been studied in this chapter with several general cases. It can be concluded that the mode count of a simply supported beam with a number of extra constraints can be estimated by the mode count of the beam without extra constraints minus the product of the number of constraints and the constraint constant δ.

Equation Section (Next)

5 EXTRUDED SECTION

The modal characteristics of the cross-section of the extruded plate are studied in this chapter. The global and local modes are identified based on an FEM model using ANSYS. The equivalent bending stiffness for global vibration of the extruded plate is developed and compared with the FEM results. The mode count of the extruded section is estimated in terms of the global and local modes, based on the study of the multi-beam system described in chapter 4. The spatially and frequency band-averaged driving point mobility is calculated using FEM and compared with the result obtained from the estimated formula.

5.1 MODAL ANALYSIS OF FEM MODEL

The extruded plate studied in this report is made of aluminium. Its basic geometric parameters were shown in Figure 1.2.

The cross-section of the extruded plate can be considered as a multi-beam system and thus the BEAM 3 element in ANSYS is chosen to represent it. The BEAM 3 element is a uniaxial element with tension, compression, and bending capabilities. The element has three degrees of freedom at each node: translations in the nodal x and y directions and rotation about the nodal z-axis. The maximum length of the element used in this FEM model is 0.01m.

A modal analysis is carried out by applying certain boundary conditions on the model. In order to obtain more global modes, symmetry and anti-symmetry boundary conditions are separately applied on the two ends of the upper and lower extruded plate. In total, four combinations of boundary conditions are analysed (shown in Figure 5.1).

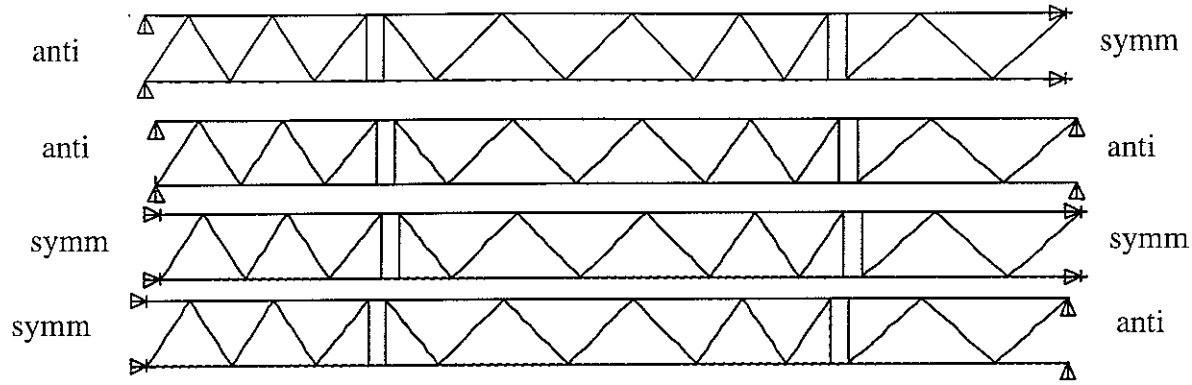

Figure 5.1 Boundary conditions applied in FEM model.

For the present model, to represent the extruded plate in plane bending, the Young's modulus E is replaced by $E/(1-\mu^2)$ where μ is the Poisson's ratio in order to account for the fact that cross-sectional contraction is prevented in one direction ('plane strain' model).

The FEM modal analysis gives the natural frequencies and mode shapes of the extruded section. For each set of boundary conditions, only the first few modes appear to be global modes. For frequencies above 470Hz, the mode shapes become complicated and local motion of a single beam begins to dominate the modes. The frequency above which local modes occur will be denoted by f_{local}. The first few modes for each boundary condition are presented in Figure 5.2 to Figure 5.5. The local modes appear first at the longest beam segment at the right-hand side of the extruded section. For this beam segment, this is its first mode. However, it can be noted that adjacent beams also vibrate to some extent. Then local modes appear at the shorter beam segments in other locations of the extruded section, as the frequency increases.

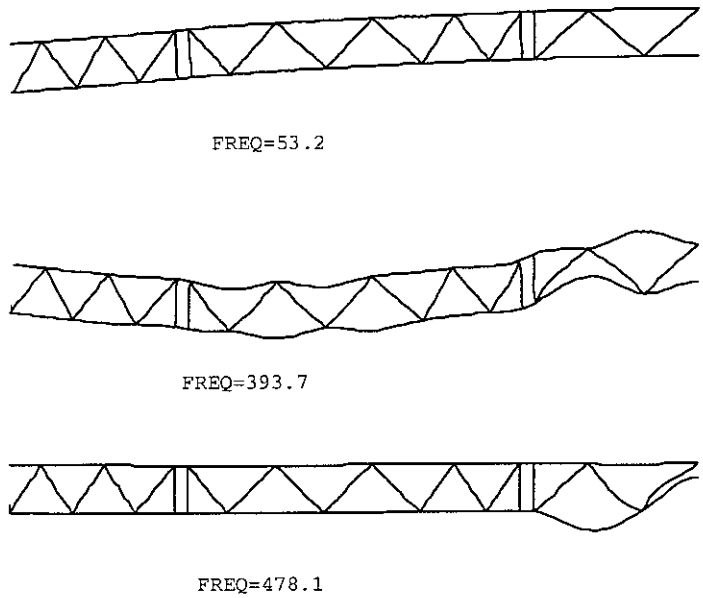

Figure 5.2. Mode shapes for the boundary condition: anti-symmetry and symmetry

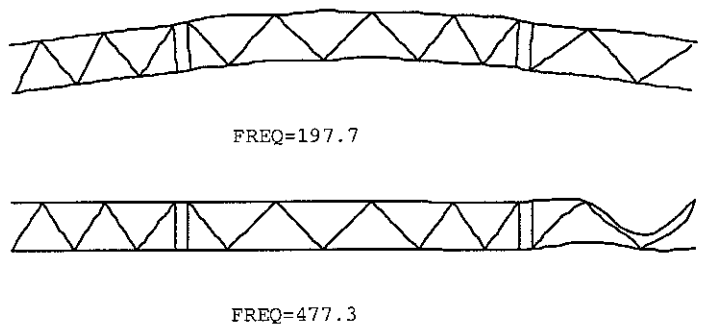

Figure 5.3. Mode shapes for the boundary condition: anti-symmetry and anti-symmetry

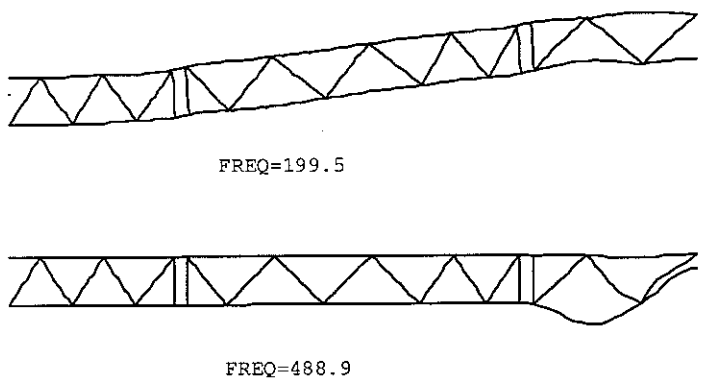

Figure 5.4 Mode shapes for the boundary condition: symmetry and symmetry

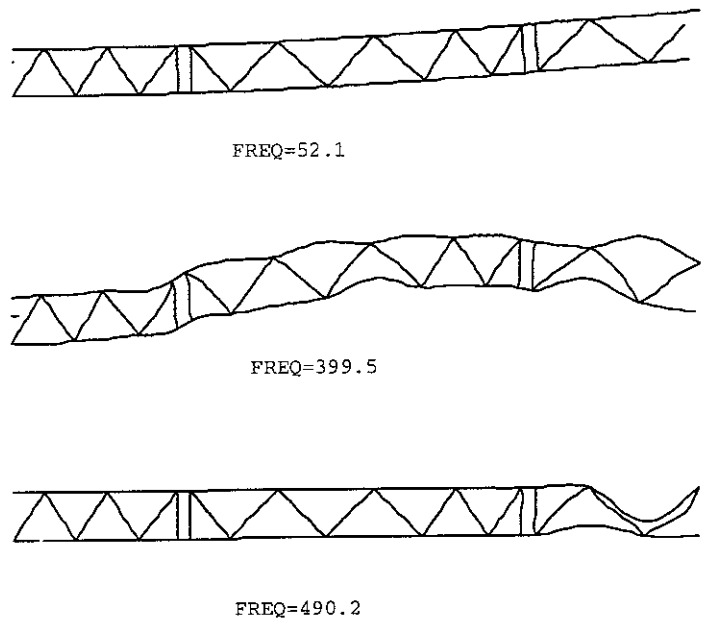

Figure 5.5 Mode shapes for the boundary condition: symmetry and anti-symmetry

5.2 EVALUATING THE MODE COUNT

To estimate the mode count of the extruded section account should be taken of the global modes and the local modes. For global modes, the extruded section can be regarded as an equivalent beam. For local modes, the extruded section can be treated as a multi-beam system.

The FEM model represents half the width of the floor. The mode count of the whole floor can be obtained by a combination of the FEM modal analysis of under the boundary conditions of antisymmetry-symmetry and antisymmetry-antisymmetry (see Figure 5.1).

5.2.1 GLOBAL MODES

To consider the extruded section as an equivalent beam, one must determine the equivalent bending stiffness for the extruded section. In such global bending motion, the stiffeners are nearly rigid and the bending induces stresses mainly in the upper and lower beams. Supposing the extruded plate is in a state of a pure bending vibration, the upper or lower beams would be either compressed or extended relative to the neutral fibre. This neutral fibre passes through the centre of gravity of the section, and actually is located at the mid-point of the section (see Figure 5.6). The stiffeners do not bear the tensile and compressive stress under the pure bending

condition and behave as rigid spacers that separate the upper and lower beams. Based on the above assumption, the second moment of area about the z axis per unit width can be calculated by

$$I_x = 2\times\left(\frac{h^3}{12}+\left(\frac{H}{2}-\frac{h}{2}\right)^2\times h\right) \tag{5.1}$$

where h is the thickness of the upper and lower plates and H is the height of the extruded plate. This is illustrated in Figure 5.7.

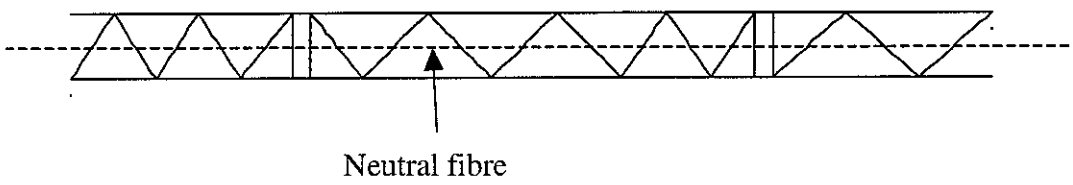

Figure 5.6 Illustration of the neutral fibre of the extruded section

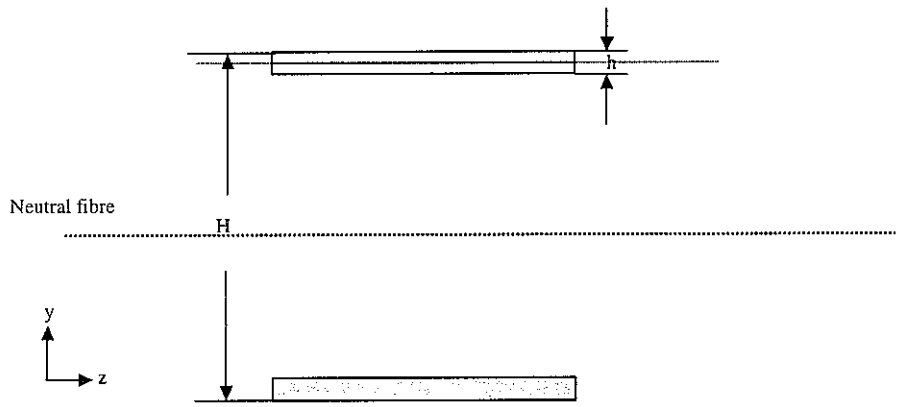

Figure 5.7 The moment of inertia of the area of the cross section

The equivalent bending stiffness can therefore be calculated by

$$B_x = E'I_x = \frac{EI_x}{1-\mu^2} \tag{5.2}$$

The dispersion relation for the equivalent beam can be expressed by

$$k_{Bg} = \omega^{\frac{1}{2}}\left(\frac{m'}{E'I_x}\right)^{\frac{1}{4}} \tag{5.3}$$

where m' is the mass per unit length, which is given by $m' = \frac{\rho h l_{tot}}{L}$, where l_{tot} is the total length of all the beam segments and L is the length of the section.

To investigate the validity of the above assumption, the bending stiffness can be determined from the FEM model using the dispersion relation of bending vibration and then compared with the result of equation (5.2). The dispersion relation of bending vibration is given by

$$k = \sqrt[4]{\frac{m'}{B}\omega^2} \tag{5.4}$$

where k is the wavenumber, m' is the mass per unit length, B is the bending stiffness of the beam and ω is the radian frequency. Taking the wavelength from the mode shape shown in Figure 5.2 to Figure 5.5, the wavenumber for the global modes can be obtained by

$$k = \frac{2\pi}{\lambda} \tag{5.5}$$

where λ is the wavelength for the global vibration.

By rearranging equation (5.4), and substituting the wavenumber and natural frequencies, the bending stiffness can be calculated. This is shown in Table 5.1. The averaged value from the first mode for each set of boundary conditions from the FEM model is 5.336×10^5 Nm^2. The value calculated by equation (5.2) is 5.369×10^5 Nm^2. The difference between the estimated formula and the FEM results is less than 1%.

Table 5.1 The wave number and bending stiffness derived from FEM analysis

Boundary conditions	Frequency (Hz)	Wavelength (m)	Wave number (rad/m)	Bending stiffness (Nm^2)
antisymmetric-symmetric	53.2	4.032	1.558	5.764×10^5
antisymmetric-symmetric	393.7	3.344	4.675	3.896×10^5
antisymmetric-antisymmetric	197.7	2.016	3.117	4.974×10^5
symmetric-symmetric	199.5	2.016	3.117	5.068×10^5
symmetric-antisymmetric	52.1	4.032	1.558	5.534×10^5
symmetric-antisymmetric	399.5	3.344	4.675	4.013×10^5

Now the mode count of the global modes can be readily obtained by using the approximate formula

$$N_g = \frac{k_{Bg} L}{\pi} - \delta_{BCg} \tag{5.6}$$

where N_g is the mode count of the global modes, k_{Bg} is the wavenumber, which can be obtained from the knowledge of the equivalent bending stiffness for the global modes and δ_{BCg} is the constant due to boundary conditions described in Chapter 2. For current case, simple supports are applied on the two ends of the extruded section (full floor) so that δ_{BCg} is 1/2.

Simple *Euler-Bernoulli* beam theory is valid at long wavelengths. At higher frequencies shear deformation and rotational inertia need to be considered. So the beam theory of *Timoshenko* is introduced for evaluation of the global mode count for high frequency. The dispersion relation of the *Euler-Bernoulli* beam is therefore modified and expressed by

$$E' I_x \beta^4 + \rho I_x \left(1 + \frac{E'}{G\kappa}\right)\omega^2 \beta^2 - \rho A \omega^2 + \frac{\rho^2 I_x}{G\kappa}\omega^2 = 0 \tag{5.7}$$

where $\beta = ik_{Timo}$, k_{Timo} is the wavenumber, κ is the *Timoshenko* shear coefficient, I_x is the second moment of area of the equivalent beam, E' is the corrected Young's modulus and G is the shear modulus. The shear modulus is given by $G = \frac{E}{2(1+\mu)}$. The value of κ is partly determined through the analysis of the mobility of joint locations using the FEM model (see section 5.3). Here, $\kappa = 0.2$ is used.

The solution of the first propagating wave* from equation (5.7) gives the wavenumber of the *Timoshenko* beam, which is represented by

$$k_{Timo} = \sqrt{\frac{\rho I_x \left(1 + \frac{E'}{G\kappa}\right)\omega^2 + \sqrt{\left[\rho I_x \left(1 + \frac{E'}{G\kappa}\right)\omega^2\right]^2 - 4E' I_x \left(-\rho A \omega^2 + \frac{\rho^2 I_x}{G\kappa}\omega^2\right)}}{2E' I_x}} \tag{5.8}$$

The global mode count of the *Timoshenko* beam can be calculated by

$$N_g = \frac{k_{Timo} L}{\pi} - \delta_{BCg} \tag{5.9}$$

---

* The solutions of equation (5.7) have two sets of waves. The first is a propagating wave. The second is a near-field wave at low frequency and propagating at higher frequency. Equation (5.8) is the first propagating wave.

Figure 5.8 shows the global mode count obtained from both equation (5.6) and (5.9). It can be seen that the *Timoshenko* beam has a similar result to that of *Euler-Bernoulli* beam below 200Hz while, above 200Hz, the mode count of the *Timoshenko* beam increases more quickly than *Euler-Bernoulli* beam. It will be shown later in section 5.2.4 that the *Timoshenko* beam is a more appropriate model for the global vibration than *Euler-Bernoulli* beam. The beam models give results that are close to the FEM results up to f_{local} which in this case is 470Hz. Above this frequency the FEM results are dominated by the local modes.

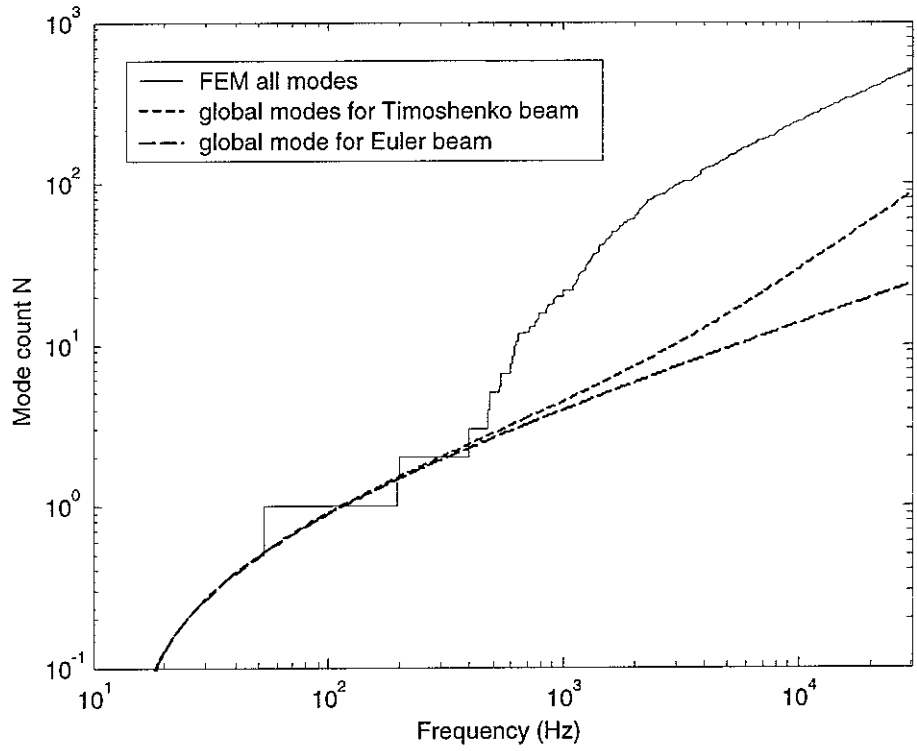

Figure 5.8 Global modes of the extruded section.

5.2.2 LOCAL MODES

The mode count for local modes can be approximately considered by treating the extruded section as a multi-beam system. In chapter 4, multi-beam systems were discussed, both finite periodic and randomly spaced, that consisted only of a single line of segments joined end-to-end. The boundary conditions concerned were also only ideal conditions such as the simple support. For the extruded section, the beam segments are not joined in a single line and the boundary conditions at the joint points are unknown. Basically, the extruded section is a complicated multi-coupled multi-beam system. However, based on the study described in the previous chapters, in which the mode count of a multi-beam system can be estimated by the mode count

of a beam with a total length of all the segments, modified to account for the constraints, the mode count for the extruded section can also be investigated in a similar way.

In order to use this method to predict the mode count for the extruded section, one must first investigate the boundary conditions between those beam segments. This can be done by checking the wavenumber for each beam segment in its local mode. For each local mode, usually only one beam segment dominates the vibration. In other words, the mode of the whole system is determined by this beam segment. The dispersion relation of the bending vibration for this beam segment must satisfy the equation (5.4), where the bending stiffness and mass per unit length refer now to the beam segment. The relation between the wavenumber and the frequency helps to understand the boundary conditions experienced by this beam segment. For example, it is well known (see also Appendix A) that the fixed-fixed boundary condition will give a first mode of a beam which has the largest wavenumber compared with other boundary conditions. Therefore, the natural frequencies of every local mode below 2000Hz directly obtained from the FEM analysis is used to calculate the wavenumber, assuming the beam to be subject to fixed-fixed boundary conditions, by using the frequency equation described in Appendix A. These results are compared with the dispersion relation for free waves in the beam segment. This is plotted in Figure 5.9. For comparison, the wavenumber estimated by assuming a pinned-pinned condition applied to each local mode is also calculated and presented in Figure 5.9.

These results show that each beam segment is in a state between the fixed-fixed boundary condition and pinned-pinned. It may be noted that intermediate simple supports on a beam lead to local modes somewhere between pinned-pinned and fixed-fixed (actually between pinned-pinned and pinned-fixed, see section 4.2.1). Therefore it is assumed, as a first approximation, that each local beam is simply supported at its ends as well as connected to its neighbours. This leads to an approximate expression for the local modes of the extruded section. It is given by

$$N_l \approx \frac{kl_{tot}}{\pi} - (m-1)\times\frac{3}{4} \tag{5.10}$$

where N_l is the mode count of the local modes, m is the number of the beam segments, l_{tot} is the total length of the beam segments. For this section (whole floor), m= 78, and l_{tot} = 7.41m.

The extruded section is different from the multi-beam system discussed in Chapter 4. It includes four simple supports at two ends, the irregularly spaced beam segments and unknown boundary conditions between them. Although these differences exist, the estimation based on equation (5.10) is of a similar form to that for the multi-beam system discussed in Chapter 4. This

estimation is the simplest one but will give a useful understanding of the dynamics of the extruded section. It also leads to potential estimation errors to some extent. Results will be compared with the FEM mode count in section 5.2.4 below.

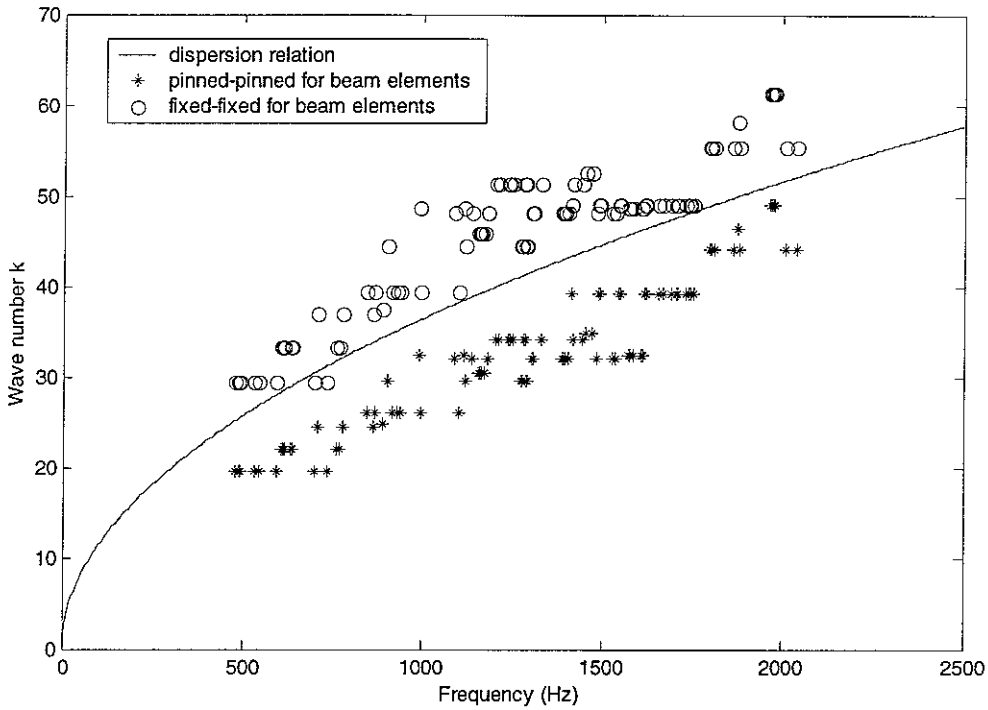

Figure 5.9 Wavenumber of the local modes of the extruded section.

5.2.3 LONGITUDINAL MODES

In order to estimate the mode count of the extruded section, for comparison with the FEM results, the longitudinal vibration must be also taken into account. The longitudinal modes can also be considered to consist of global and local modes. The local modes occur when a half wavelength would fit within a single beam segment. For the longest beam segment in the extruded section, 0.16m, the first mode would occur at 16250Hz for the wave speed 5200m/s. For shorter beam segments, the first mode would occur at a higher frequency. The local longitudinal modes may therefore be ignored when the mode count for the whole system is considered. The global longitudinal modes may be considered as the modes of a simple rod with the length of the extruded section. The corresponding mode count is given by

$$N_L = \frac{k_L L}{\pi} \tag{5.11}$$

where N_L is the longitudinal mode count, k_L is the wavenumber of the longitudinal vibration and L is the length of the extruded section.

Figure 5.10 shows the longitudinal mode count for the extruded section. It can be seen that the longitudinal mode count has a comparably small contribution to that of the whole system.

A second set of global longitudinal modes exists in which the two outer beams vibrate in opposite directions on the shear stiffness of the intermediate 'layer'. However, these modes have not been included here as they occur at high frequency and will have even smaller contributions to the mode count than the modes in Figure 5.10.

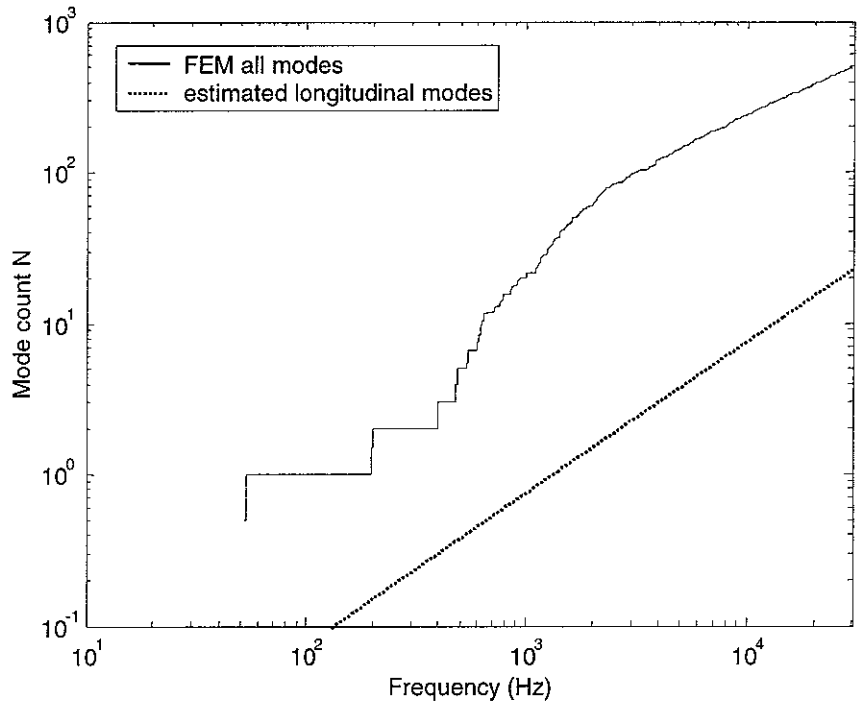

Figure 5.10 The longitudinal mode count of the extruded section.

5.2.4 MODE COUNT FOR EXTRUDED SECTION

Now the mode count for the extruded section will be estimated and compared with the results of the FEM model. The mode count of the extruded section can be approximately calculated by

$$N = \begin{cases} N_L + N_g & f < f_{local} \\ N_L + N_g + N_l & f \geq f_{local} \end{cases} \tag{5.12}$$

where N_L is the mode count for the longitudinal vibration from equation (5.11), N_g is the mode count for the global bending modes from equation (5.9) and N_l is the mode count for the local bending modes from equation (5.10).

Figure 5.11 presents the mode count estimated by equation (5.12) and that obtained from the FEM model. Figure 5.12 presents the same curves as Figure 5.11 but with logarithmic axes so that the difference at low frequency can be clearly seen. The estimated value is larger than that obtained from FEM above 500Hz. The difference between these two curves is plotted against frequency in Figure 5.13. The averaged difference is 12.5.

If a fixed boundary condition is considered to exist between the beam segments in the extruded section in place of the pinned boundary condition, the local modes can be predicted by

$$N_l = \frac{kl_{tot}}{\pi} - (m-1) \tag{5.13}$$

The corresponding results are presented in Figure 5.14 to Figure 5.16. The average difference between the estimated and FEM mode count is – 6.2.

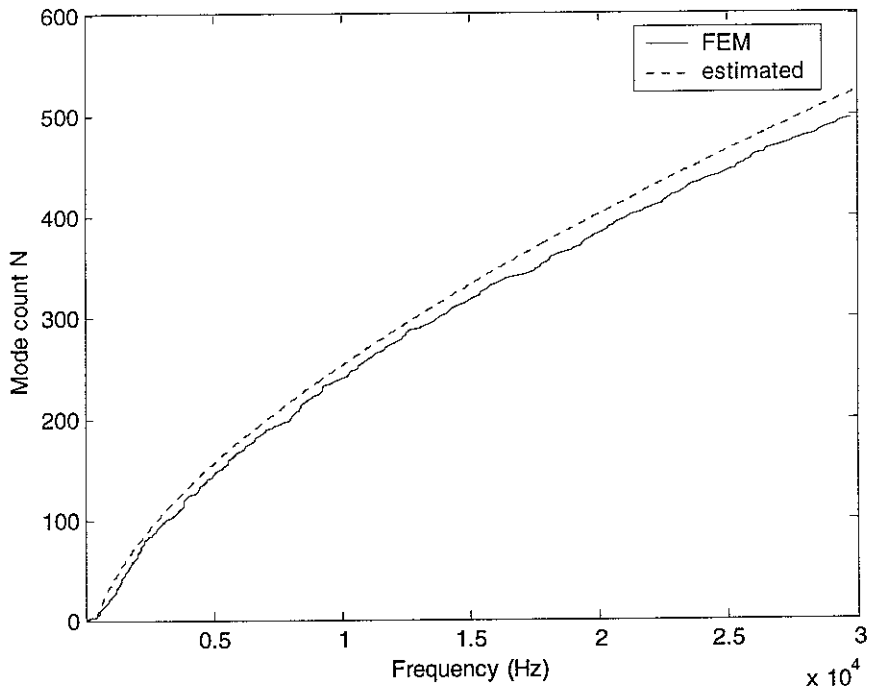

Figure 5.11 Mode count of the extruded section for the whole floor. (simple support condition supposed between beam segments).

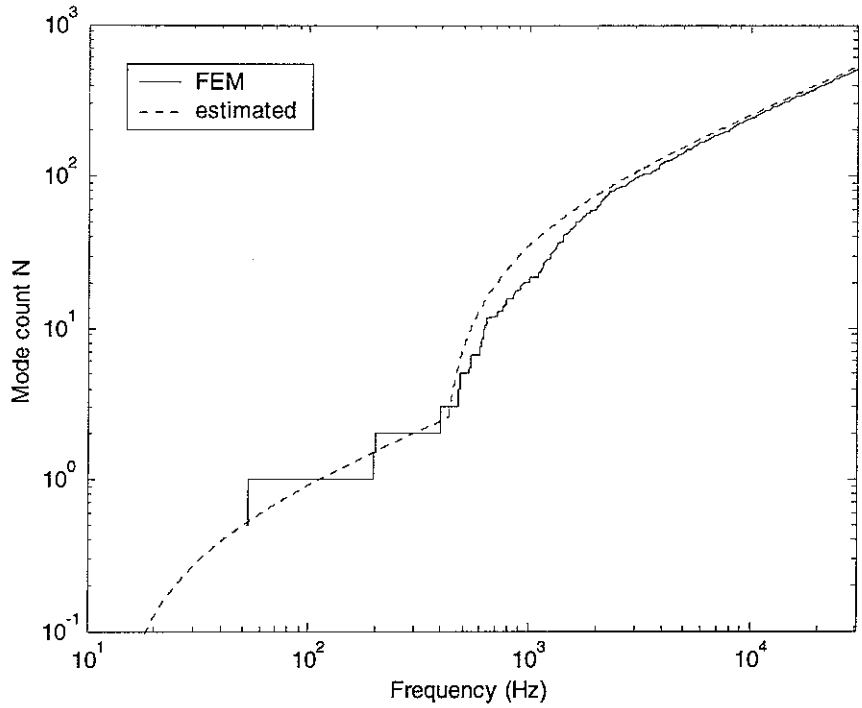

Figure 5.12 Mode count of the extruded section for the whole floor.
(simple support condition supposed between beam segments).

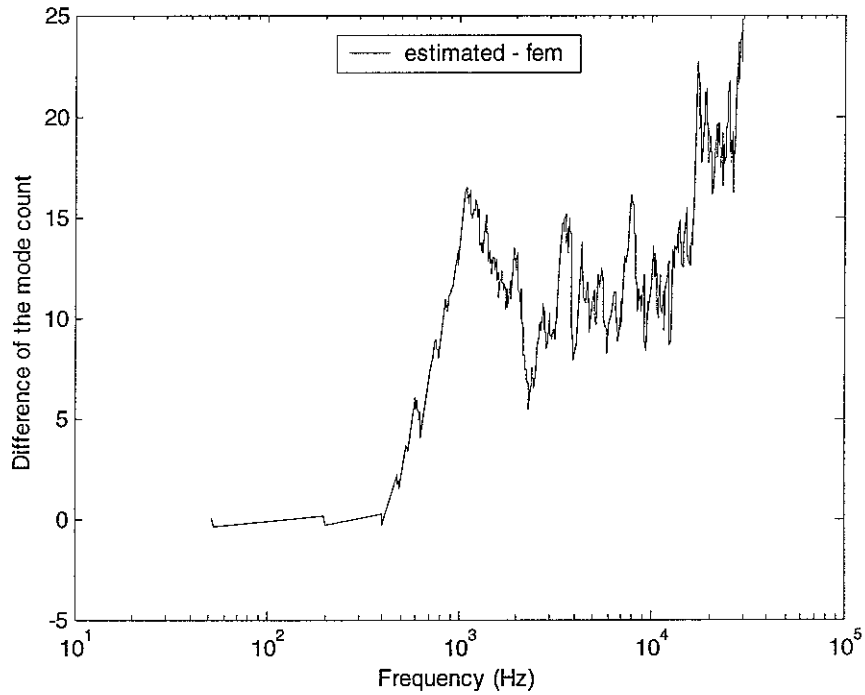

Figure 5.13 The difference between the estimated and FEM mode count.
(simple support condition supposed between beam segments).

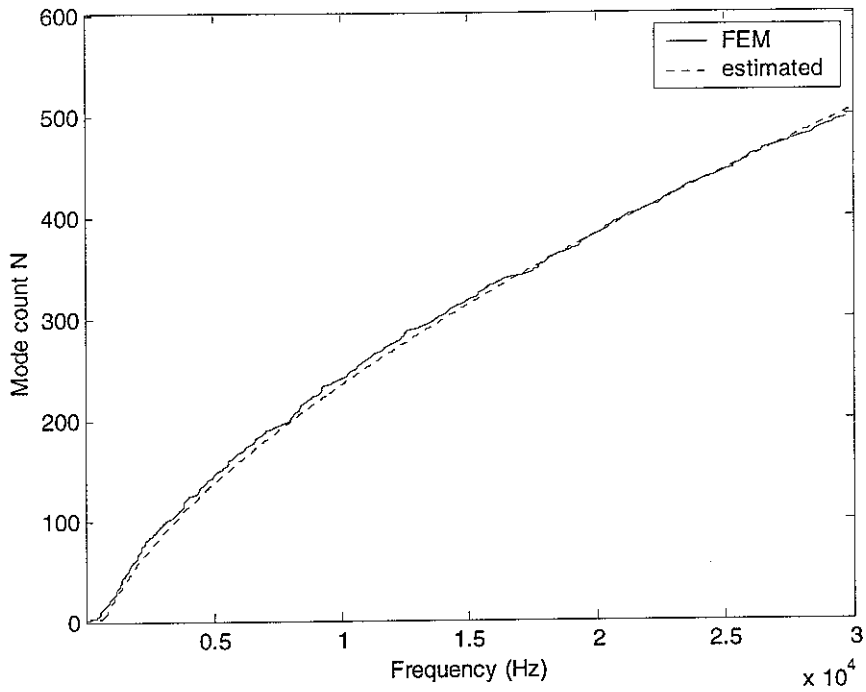

Figure 5.14 Mode count of the extruded section for the whole floor. (fixed conditions supposed between beam segments).

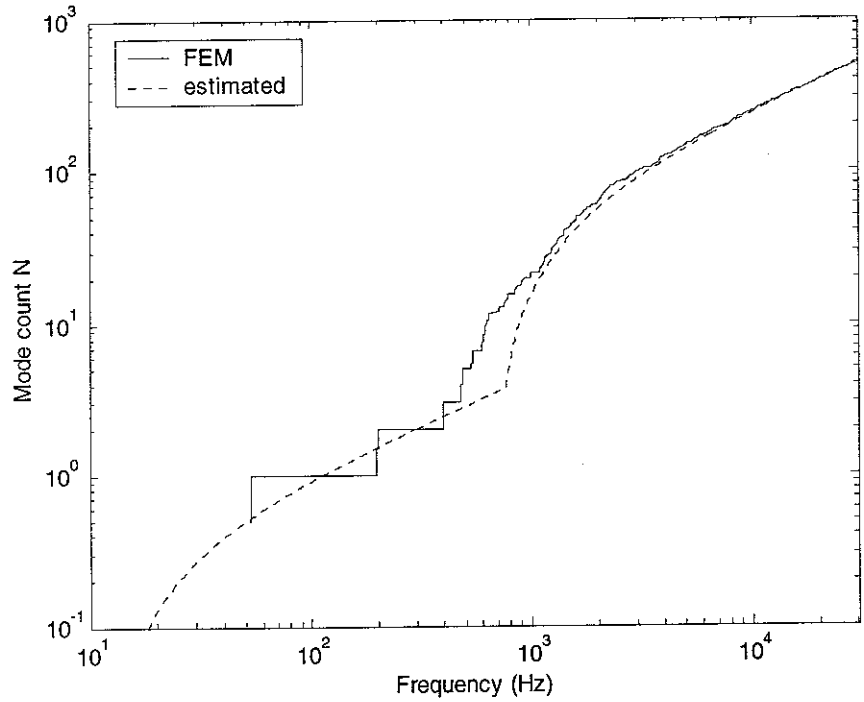

Figure 5.15 Mode count of the extruded section for the whole floor. (fixed conditions supposed between beam segments).

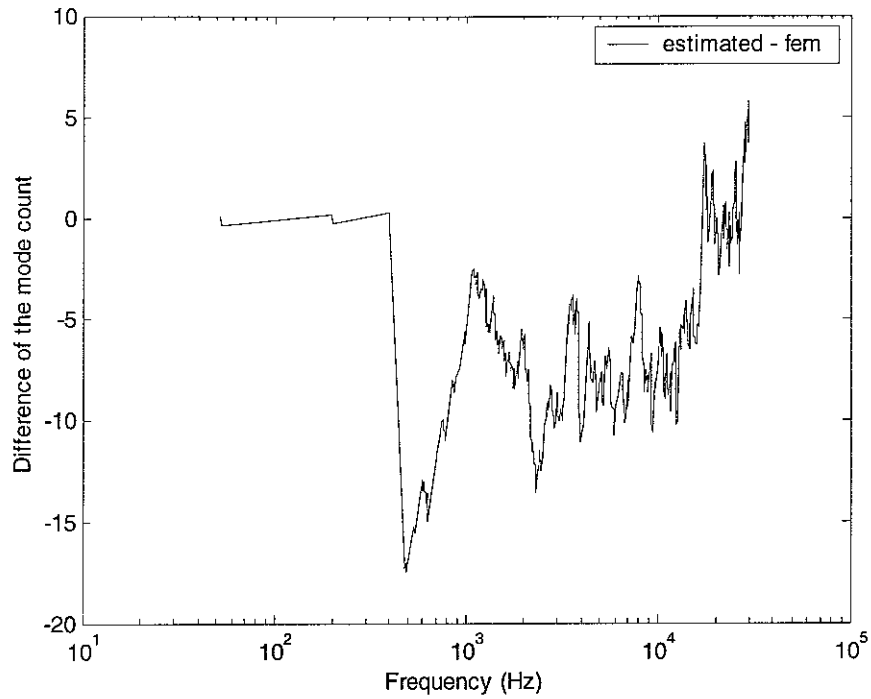

Figure 5.16 The difference between the estimated and FEM mode count. (fixed conditions supposed between beam segments).

It can be concluded that the actual constraint between beam segments of the extruded section is somewhere between simply supported and fixed conditions. From the difference between the estimated value and that from the FEM, the fixed conditions are more appropriate to the real situation than simple supports for frequencies above 1kHz, but at lower frequencies 400 to 700Hz, the simple support is a better approximation.

This shows that the conclusion drawn from the one-dimensional system consisting of a single line of segments with either intermediate simple supports or fixed constraints cannot provide a satisfactory agreement when it is applied in a complicated real structure, the extruded section. The extruded section is constructed of a set of beam segments, each of which is coupled with its neighbouring segments. The coupling degrees of freedom include longitudinal and transverse displacement and rotation. For such a multi-coupled system, further separate investigations are really required.

Nevertheless the boundary condition constant δ experienced by the beam segments can be identified through rearranging equation (5.12). The actual mode count is given by

$$N = N_L + N_g + N_l = \frac{k_L l_{tot}}{\pi} + \frac{k_{Bg} L}{\pi} - \delta_{BCg} + \frac{k_B l_{tot}}{\pi} - (m-1)\times\delta_{BC} \qquad f \geq f_{local}$$

If the mode count obtained from the FEM model is substituted into the left-hand of the above equation, the δ_{BC} can be calculated by

$$\delta_{BC} = \frac{\left(N_{FEM} - \frac{k_L l_{tot}}{\pi} - \frac{k_{Bg} L}{\pi} + \delta_{BCg} - \frac{k_B l_{tot}}{\pi} \right)}{(m-1)} \qquad f \geq f_{local} \qquad (5.14)$$

The results of equation (5.14) are presented in Figure 5.17. It can be seen that the constant of the boundary conditions varies with frequency. For frequencies between 500Hz and 1000Hz, δ roughly changes from 0.75 to 0.95. This change might explain the disagreement between 500Hz and 1000Hz in the prediction of the mode count by using fixed or pinned boundary conditions. The pinned boundary conditions have a better agreement in the prediction for the frequencies from 500Hz to 700Hz because δ is close to 0.75 in this frequency range. Both cases give disagreement from 700Hz to 1000Hz because δ is between 0.75 and 1. Above 1000Hz, δ fluctuates around a mean value of about 0.9, which is closer to a fixed boundary condition. Above 16kHz, the estimated value of δ exceeds 1 but it should be noted that at these high frequencies the wavelength of the global modes becomes shorter than twice the length of an individual beam segment, so that the model for global modes becomes inappropriate. This will affect this estimate.

During the study of δ, it has been found that the results are very sensitive at high frequency to the value of κ used for the global modes. It is also noted that the model of a *Euler-Bernoulli* beam for the global modes is not appropriate. Figure 5.18 shows the result obtained from different values of κ and the *Euler-Bernoulli* beam. Above 7kHz, the result from $\kappa = 0.1$ would not be appropriate as $\delta > 1$. Between 1kHz to 16kHz, the average result of δ for $\kappa = 0.2$ can be approximated to be 0.9, shown by the solid line.

It may be noted that the concept of a frequency-dependent boundary condition is consistent with the cases of a mass or stiffness considered earlier, although in the present case δ increases with increasing frequency whereas in the previous cases δ decrease with increasing frequency.

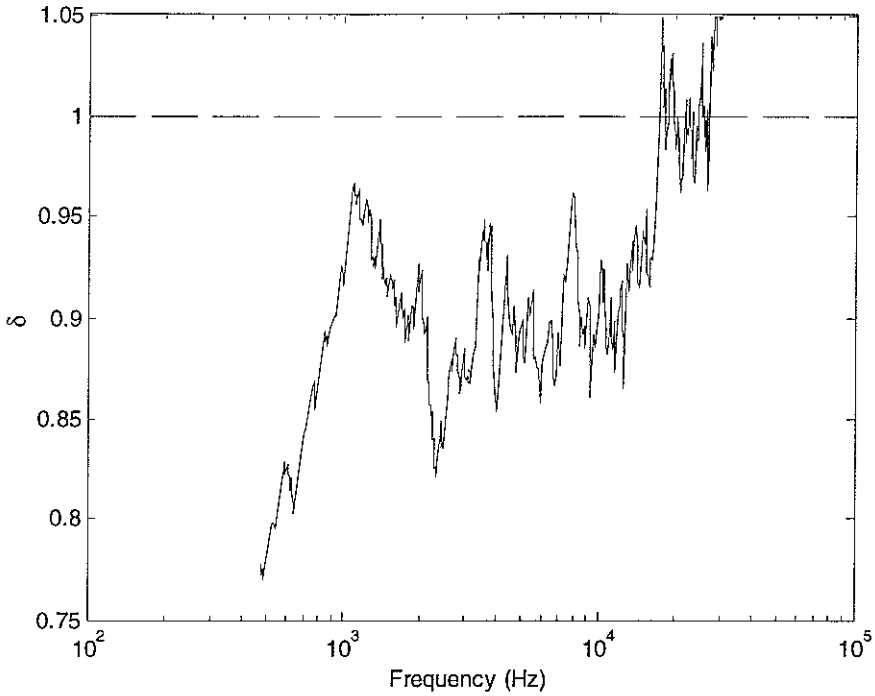

Figure 5.17 Constants of boundary conditions as a function of frequency.

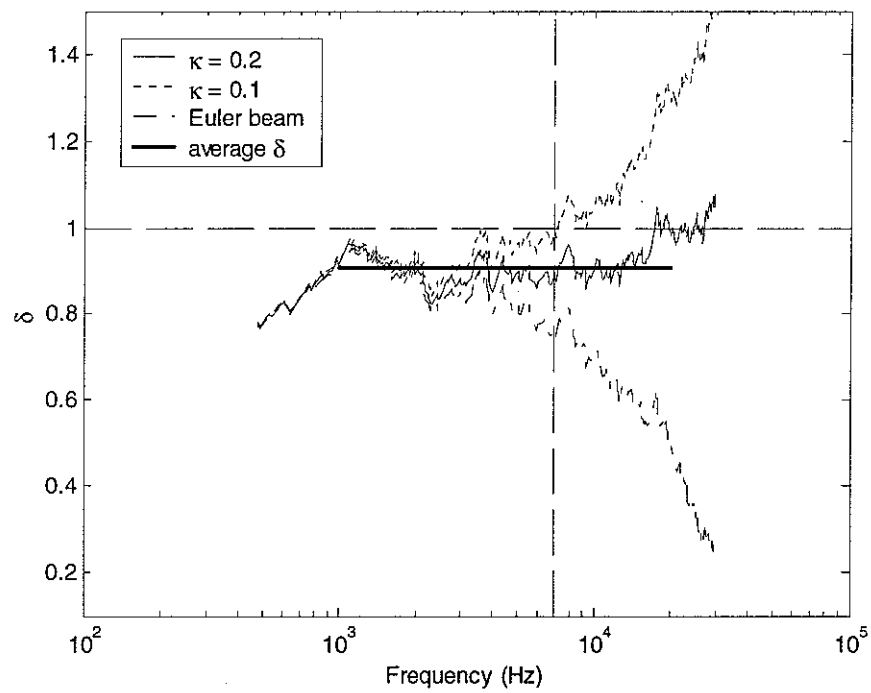

Figure 5.18 The result of δ obtained from different models.

5.3 MODAL DENSITY AND DRIVING-POINT MOBILITY

In practice, the spatially averaged driving point mobility for a complicated structure is required since it can be used to calculate the power input to the system. Cremer and Heckl [6] give the following approximate expression to calculate the frequency band averaged real part of the driving point mobility

$$\mathrm{Re}\{Y\} = \frac{\pi}{2m} n(\omega) \tag{5.15}$$

where m is the mass of the system and $n(\omega)$ is the modal density of the system.

The modal density is the slope of the mode count function against frequency. In the case of the extruded section, although the mode count for local modes is different from the single equivalent beam with the same total length as all the beam segments, the slope (modal density) at frequencies above 1kHz is similar. Using this idea, the modal density can be approximately obtained by the differentiation of equation (5.12). Equation (5.12) is given by

$$N = N_L + N_g + N_l = \begin{cases} \dfrac{k_L L}{\pi} + \dfrac{k_{Bg} L}{\pi} - \delta_{BCg} & f < f_{local} \\ \dfrac{k_L L}{\pi} + \dfrac{k_{Bg} L}{\pi} - \delta_{BCg} + \dfrac{k_B l_{tot}}{\pi} - (m-1) \times \delta_{BC} & f \geq f_{local} \end{cases} \tag{5.16}$$

where $k_B = \omega^{\frac{1}{2}} \left(\dfrac{\rho h}{E'I} \right)^{\frac{1}{4}}$ is the wavenumber of bending vibration of the beam segment, k_{Bg} is the wavenumber of the global bending vibration, l_{tot} is the total length of the beam segment of the extruded section and $k_L = \dfrac{\omega}{c_L}$ is the wavenumber of longitudinal vibration.

The modal density of the extruded section now can be given by

$$n(\omega) = \frac{dN}{d\omega} = \begin{cases} \dfrac{L}{c_L \pi} + \dfrac{k_{Bg} L}{2\pi\omega} & f < f_{local} \\ \dfrac{L}{c_L \pi} + \dfrac{k_{Bg} L}{2\pi\omega} + \dfrac{k_B l_{tot}}{2\pi\omega} - (m-1) \dfrac{d\delta_{BC}}{d\omega} & f \geq f_{local} \end{cases} \tag{5.17}$$

which includes four components: longitudinal, global bending, local bending and boundary conditions experienced by all beam segments. The first two items have only a small contribution to the modal density above 470Hz since the local bending dominates the whole system above this frequency. δ_{BC} is represented by a function of frequency as shown in Figure 5.17. From

500Hz to 1kHz, δ_{BC} changes approximately linearly from 0.78 to 0.93. At frequencies above 1kHz, δ_{BC} is approximately constant. Therefore, $\frac{d\delta_{BC}}{d\omega}$ or $\frac{d\delta_{BC}}{df}$ can be approximately expressed by

$$\frac{d\delta_{BC}}{df} = 2\pi \frac{d\delta_{BC}}{d\omega} = \begin{cases} 0.15/500 & 500\text{Hz} < f < 1\text{kHz} \\ 0 & f > 1\text{kHz} \end{cases} \tag{5.18}$$

The result calculated from equation (5.17) is compared with that from the FEM modal analysis, which is obtained by counting the number of the modes in each one-third octave band. This is presented in Figure 5.19. The curves presented in Figure 5.19 are in terms of *n(f)*, which is given by

$$n(f) = 2\pi n(\omega) \tag{5.19}$$

Figure 5.19 presents the estimated modal densities by using both the *Timoshenko* and *Euler* beam for the global vibration. The estimated results give a good agreement above f_{local}. It can be noted that only some slight differences occur between both beam models. This demonstrates that the modal density is not sensitive to which model is chosen for the global vibration. The modal density above 500Hz is dominated by the local vibration.

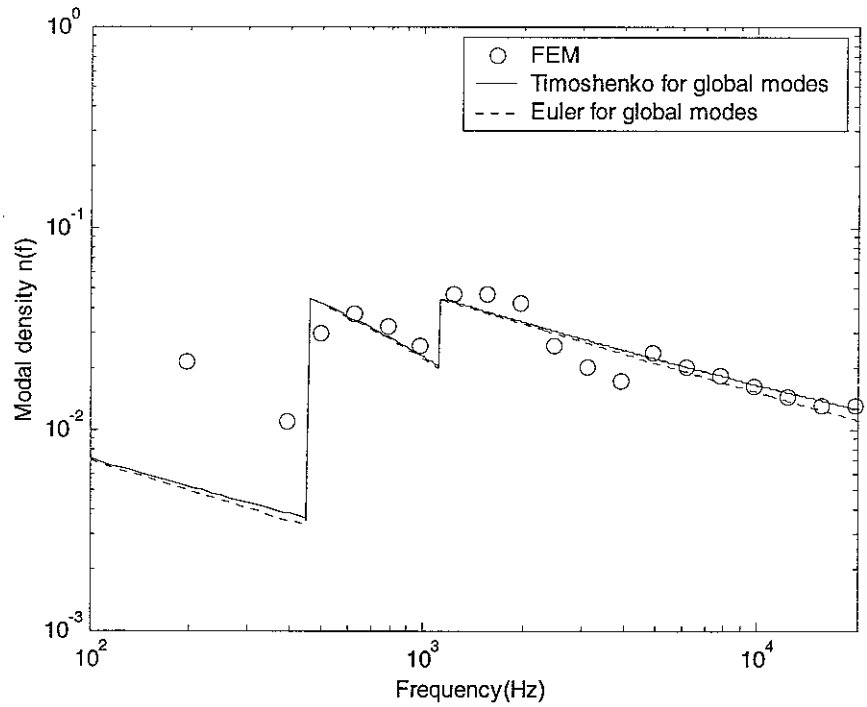

Figure 5.19 The modal density of the extruded section

The real part of the driving point mobility can thus be calculated approximately from equation (5.15) by using equation (5.17). The estimated result is compared with that from the FEM model in Figure 5.20. The result shows a good agreement in the frequency range above 500Hz where local modes occur. The FEM analysis is based on the average of the real part of the driving point mobility calculated for 27 points on the upper plate of the extruded section, in which 17 points are located on the beam segments away from the joints and the others are at joints. The value of the damping loss factor used is 0.2. There are large variations between the mobilities at these various points, as shown by the range in Figure 5.20. The estimated result based on equation (5.15) is reliable for the mean value. Because of the truncation of the modal summation in the FEM analysis, a small systematic difference occurs at frequencies near to the upper limit. In the analysis of the FEM model, a smaller value of the damping loss factor 0.06 is also calculated. The results do not have too much difference from that of value 0.2, as shown in Figure 5.21.

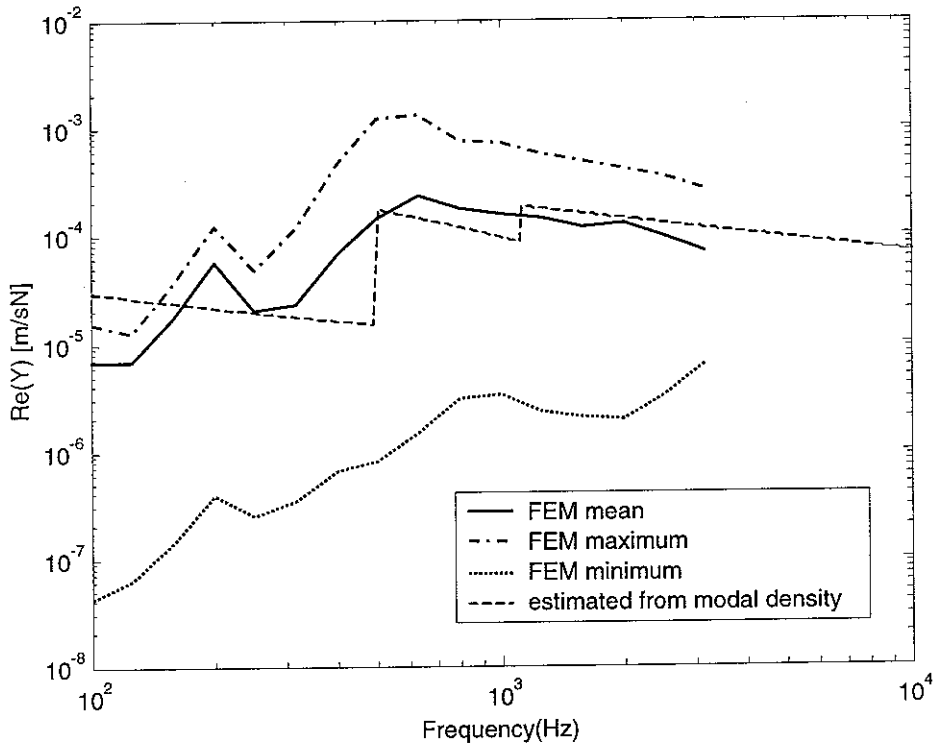

Figure 5.20 Comparison between the estimated mobility and FEM.

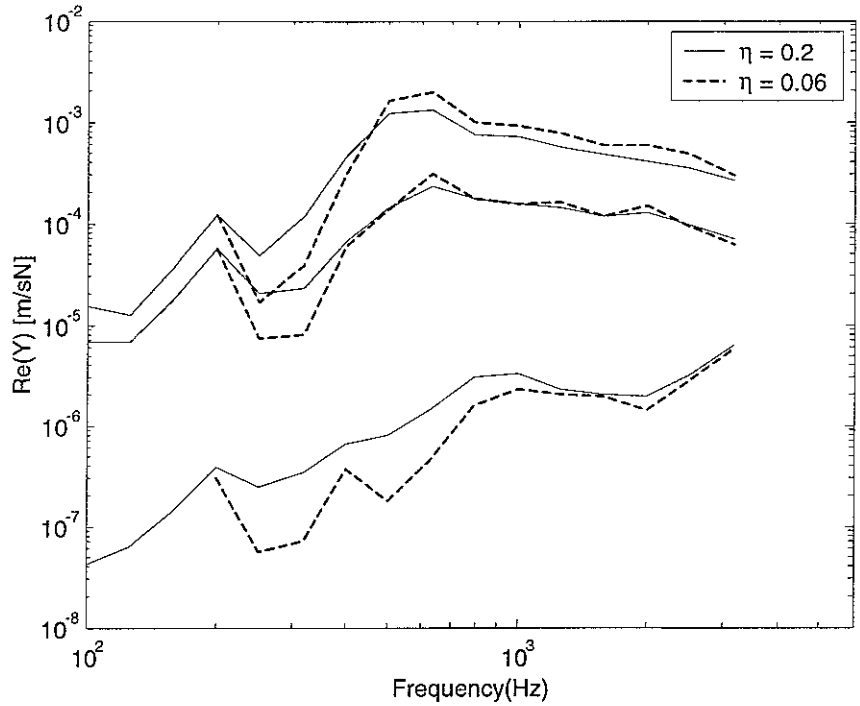

Figure 5.21 Mobility of different damping values.

It may be anticipated that the mobility at the joint points will be much lower than at intermediate points because their responses depend only on the global vibration. Using the equivalent beam for the global modes, the mobility can also be evaluated by

$$\mathrm{Re}\{Y\} = \frac{k_{Bg}}{4m'\omega} \tag{5.20}$$

where k_{Bg} is the wave number of the global bending vibration and m' is the mass per unit length of the equivalent beam.

The results of equation (5.20) are presented in Figure 5.22. Compared with the results obtained from the FEM analysis, the *Euler-Bernoulli* beam model is not appropriate. Therefore, the *Timoshenko* thick beam should be introduced at high frequency for global modes. For a thick beam, the mobility can be calculated by the following formula from [6][†]

[†] Note that a typing error in [6] has been corrected and that $h^2/12$ has been replaced by I_x/A.

$$Y = \frac{k_{Bg}}{2\omega m'(1+j)} \frac{\left(\sqrt{1-\frac{E'}{G^*}\left(\frac{k_{Bg}{}^2 I_x}{A}\right)^2} + j\frac{E'}{G^*}\frac{k_{Bg}{}^2 I_x}{A}\right)}{\sqrt{\sqrt{1-\frac{E'}{G^*}\left(\frac{k_{Bg}{}^2 I_x}{A}\right)^2} + j\left(\frac{E'}{G^*}+1\right)\frac{k_{Bg}{}^2 I_x}{2A}}} \tag{5.21}$$

where $G^* = \kappa G$, in which $\kappa = A_e/A$ is the *Timoshenko* shear coefficient and G is the shear modulus. The shear modulus is given by $G = \frac{E}{2(1+\mu)}$. A_e is the cross-sectional area effective in shear and is unknown for the extruded section because of the irregular cross-section. A is the total area of the cross-section. I_x is the second moment of area of the equivalent beam. The wavenumber k_{Bg} in equation (5.21) is that applying to the *Euler-Bernoulli* beam formulation.

In order to use equation (5.21), a suitable value for κ is needed. Several values of κ have been used in (5.21), and the results are compared with those from the FEM model. Figure 5.22 shows the results. It can be seen that 0.1 gives the closest agreement. In section 5.2.4, however, the different values of κ lead different results in the prediction of the mode count. $\kappa = 0.1$ only gives physically meaningful results below 7kHz. $\kappa = 0.2$ gives a more acceptable result for the frequency in the whole audio range and has therefore been adopted.

From Figure 5.22, it can be seen that the mean mobility of the whole system at low frequency is similar to that at the joint locations, as it is governed by global vibration. At high frequency, the vibration of whole system is dominated by local modes and the mobility can be predicted from the local modes. The global modes have only a small contribution to the modal density of the whole system here. The formula for the thick beam with a suitable value of κ gives a better agreement to the mobility at the joint locations. This confirms that the thick beam model is more appropriate than the thin beam model above 200Hz.

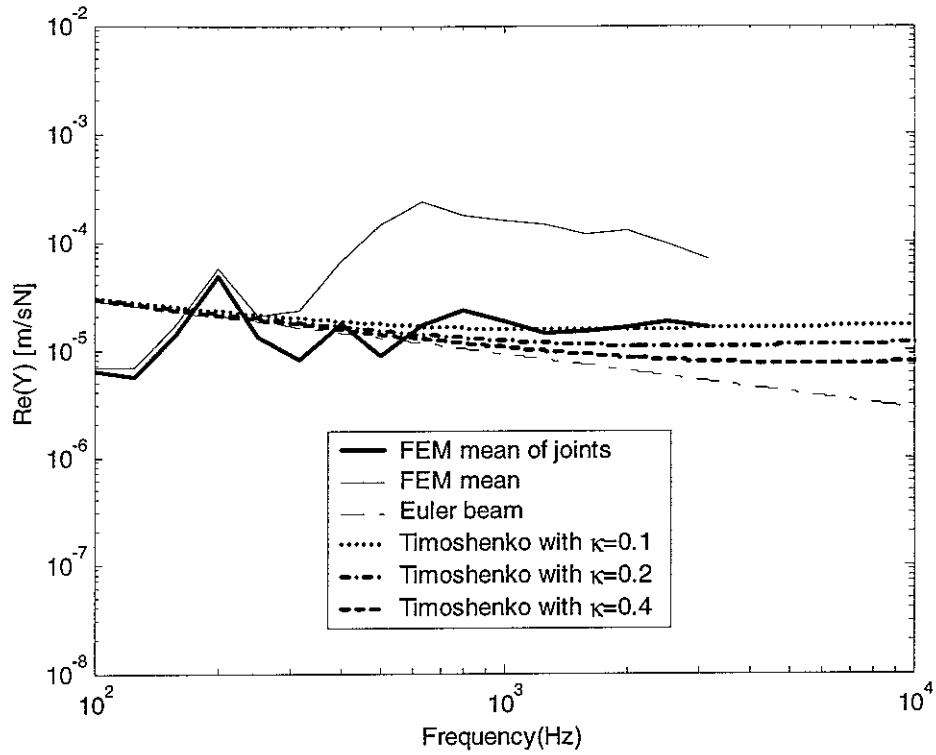

Figure 5.22 Mobility of the joint points from the FEM and estimated values

5.4 CONCLUSION

The mode count of the extruded section is more complicated than the multi-beam system in a single line described in Chapter 4. An approximate method has been developed. Some small differences are found when the estimated value is compared with the result of the FEM analysis. Despite this disagreement in the prediction of the mode count, the average driving point mobility gives a good agreement for positions dominated by local modes. This illustrates the important point in structural vibration that the mode count depends on the boundary condition but the modal density is largely independent from boundary conditions and proportional to length, area or volume of the system (unless the boundary conditions themselves depend on frequency).

6 CONCLUSION

The mode count of one-dimensional subsystems has been investigated. A simple relationship has been shown between the mode count and the boundary conditions. A free boundary has no effect on the mode count of the system. For longitudinal vibrations, a fixed boundary constraint adds to the mode count by $-\frac{1}{2}$. For bending vibrations, which have two coupling degrees of freedom, a sliding constraint adds the mode count by $-\frac{1}{4}$, a simple support condition by $-\frac{3}{4}$ and a fixed boundary constraint by -1. For more general boundary conditions, here in particular a point mass and a point spring, the boundary effect on the mode count is frequency-dependent. A mass tends to be a free condition at low frequency and to be a simple support at high frequency. A spring, conversely, tends to be a simple support at low frequency and to be a free condition at high frequency.

For multi-beam systems in a single line, the mode count of the system can be estimated by the mode count of a long beam without any extra constraints minus the sum of the constraint constants. This conclusion for the multi-beam system leads to an approximation that can be used for the investigation of an extruded section. Although small errors occur in the prediction of the mode count for the extruded section, as the constraints are neither simple supports nor fully fixed, the modal density and average driving point mobility derived from this model show good agreement with FEM analyses. This demonstrates that the modal density is largely independent of the boundary conditions whereas the mode count is dependent on the boundary conditions. For complicated structures like the extruded plate at high frequencies, a point source of excitation is likely to be affected very little by the boundary conditions of the whole system on average. The response of the extruded section at high frequency (above f_{local}) can be predicted by the modal character of the beam segment. At low frequency, the global vibration is dominant, which can be represented as an equivalent beam.

The concepts and results developed in this report have been used in investigations into the mode count, modal density and the response of the section of the extruded plate without damping. They may have use in analyses of other complicated structures. The next step will be to extend the analysis to a two-dimensional plate system.

REFERENCES

1. P. Geissler and D. Neumann 1999 *Proceeding of the 1999 ASME Design Engineering Technical Conference*, Las Vegas, Nevada, paper no. DETC/VIB-8192. Modelling extruded profiles for railway coaches using SEA.
2. R. H. Lyon and R. G. DeJong 1995 *Theory and Application of Statistical Energy Analysis.* London: Butterworth-Heinemann. See page136-137.
3. D.J. Mead 1994 *Journal of Sound and Vibration* 171(5), 695-702. Waves and modes in finite beams: application of the phase-closure principle.
4. D.J.Mead 1975 *Journal of Sound and Vibration* 40(1), 1-18. Wave propagation and natural modes in periodic systems: I. Mono-coupled systems.
5. D.J.Mead 1975 *Journal of Sound and Vibration* 40(1), 19-39. Wave propagation and natural modes in periodic systems: II Multi-coupled systems, with and without damping.
6. L. Cremer, M. Heckl and E. E. Ungar 1988 *Structure-borne Sound.* Berlin: Springer-Verlag; second edition.

APPENDIX A

The natural modes and mode count of different boundary conditions for a single beam are listed in Table A.1. The mode count is calculated by

$$N = \frac{kL}{\pi} + \delta_{BC}$$

where $\delta_{BC} = 1 - \delta_L - \delta_R$. δ_L and δ_R are shown in Table 2.1.

Table A.1 Natural modes and mode count of single beam system

Boundary conditions	*Frequency equation*	δ_L	δ_R	$\delta_{BC} = 1 - \delta_L - \delta_R$	*Mode count* N
Free-free	$kL = (n - \frac{3}{2})\pi$	0	0	1	$\frac{kL}{\pi} + 1$
Free-sliding	$kL = (n - \frac{5}{4})\pi$	0	1/4	3/4	$\frac{kL}{\pi} + \frac{3}{4}$
Free-pinned	$kL = (n - \frac{3}{4})\pi$	0	3/4	1/4	$\frac{kL}{\pi} + \frac{1}{4}$
Free-fixed	$kL = (n - \frac{1}{2})\pi$	0	1	0	$\frac{kL}{\pi}$
Sliding-sliding	$kL = (n-1)\pi$	1/4	1/4	1/2	$\frac{kL}{\pi} + \frac{1}{2}$
Sliding-pinned	$kL = (n - \frac{1}{2})\pi$	1/4	3/4	0	$\frac{kL}{\pi}$
Sliding-fixed	$kL = (n - \frac{1}{4})\pi$	1	1/4	-1/4	$\frac{kL}{\pi} - \frac{1}{4}$
Pinned-pinned	$kL = n\pi$	3/4	3/4	-1/2	$\frac{kL}{\pi} - \frac{1}{2}$
Pinned-fixed	$kL = (n + \frac{1}{4})\pi$	3/4	1	-3/4	$\frac{kL}{\pi} - \frac{3}{4}$
Fixed-fixed	$kL = (n + \frac{1}{2})\pi$	1	1	-1	$\frac{kL}{\pi} - 1$